could be suppressed by the IFNβ treatment to the level of normal HFKs (Fig. 6). The number of BrdU-positive cells in the upper layers of epithelium was decreased with IFNβ treatment (Fig. 7, BrdU). As compared with IFNβ, the moderate but significant suppression could be also observed with TGFβ. In contrast, the TNFα could not suppress hyperplasia formation and it activated the invasive potential of the epithelial cells. The number of BrdU-positive cells was rather increased with TNFα. These results indicated that IFNβ treatment had an apparent suppressive effect on virus-induced hyperplasia. The results also raised the possibility that TNFα treatment accelerated virus-induced tumorigenesis.

Next, the effect of the cytokine treatment on the vegetative viral replication was analyzed. The amplification of viral DNA at the upper layer of epithelium was suppressed by the treatment of IFNβ and TGFβ (Fig. 7, ISH). On the other hand, TNFα treatment activated viral DNA amplification in the broad area of the epithelium. These observations indicated that both IFNβ and TGFβ could suppress the late phase in the HPV lifecycle and TNFα treatment had the opposite effect on it.

It is considered that the viral oncoproteins E6 and E7 are responsible for virus-induced hyperplasia.[31] We examined the effects of cytokines on the status of p53 and pRb in the raft culture in order to estimate the expression levels of E6 and E7, respectively. The expressions of p53 and pRb were decreased in the epithelial layer of the $HFK_{p18FLneo}$ raft culture as compared to those of normal HFKs (Fig. 7, p53 and pRb). It was supposed that this decrement was caused by the E6 and E7 expressed moderately in $HFK_{p18FLneo}$. IFNβ treatment recovered p53 expression at the middle layers of epithelium, although TGFβ did not modify the p53 status. TNFα enhanced p53 expression in the epithelium broadly. pRb expression was slightly recovered by all three cytokine treatments. These results indicated that the cytokines affected the expressions of p53 and pRb, although their relation to the antiviral effect remains unclear.

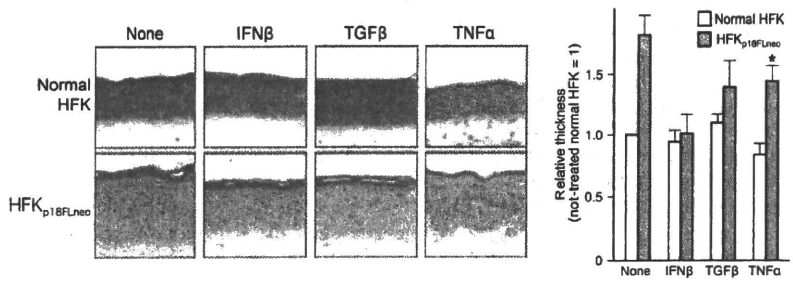

Fig. 6. Effects of cytokines on the raft culture constructed with human foreskin keratinocyte (HFK)$_{p18FLneo}$. Effects of cytokine treatments on the raft culture organized with normal HFKs or $HFK_{p18FLneo}$ were examined. Frozen-sections of the raft culture were fixed with 4% paraformaldehyde and stained with H&E. The thickness of the epidermis was estimated by microscopic analysis with an image analysis application (AxioVision; Carl Zeiss Vision), and the relative values are indicated as a bar chart (thickness of not treated normal HFK set as 1.0; average value, 95 μm). The value is the average of at least three independent experiments and the SD is indicated. Note that the epidermis of the $HFK_{p18FLneo}$ treated with tumor necrosis factor (TNF)-α exhibited the invasion phenotype; therefore, the thickness of it could not be measured precisely (indicated with an asterisk).

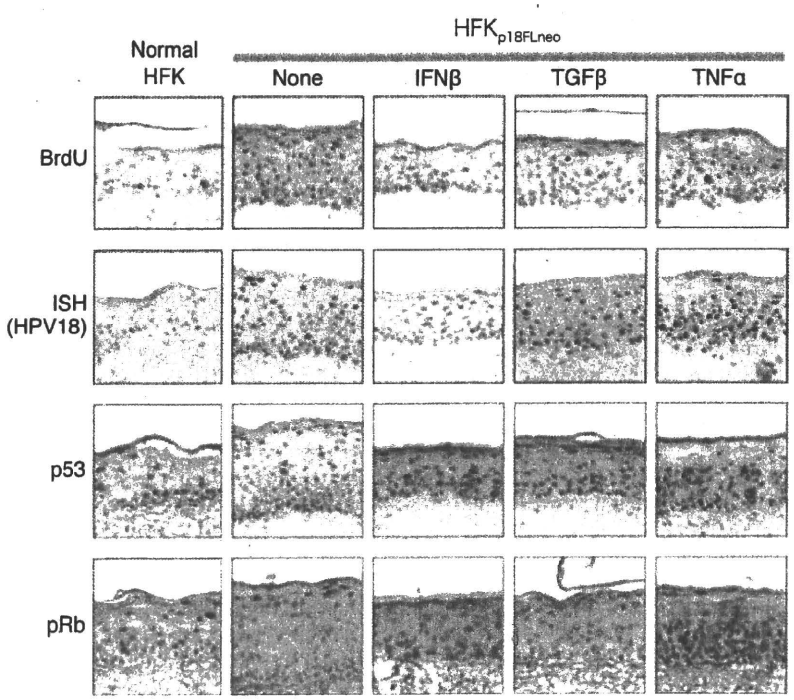

Fig. 7. The effects of cytokine treatments on human papillomavirus (HPV) replication. Effects of cytokine treatments on HPV replication and on cellular status were examined by using the raft culture. The DNA synthesis of the cells was monitored by the uptake of BrdU. Incorporated BrdU was detected by immunohistochemistry (IHC) with anti-BrdU antibody. HPV-DNA was detected by *in situ* hybridization (ISH) with DIG-labeled 18L1 probe (ISH). The expressions of p53 and pRb in the raft culture were monitored by IHC with specific antibodies (p53 & pRb).

doi: 10.1111/j.1349-7006.2009.01411.x
© 2009 Japanese Cancer Association

Discussion

A novel HPV replicon. We constructed a new replicon of HPV by integrating several improvements for the stable maintenance of the replicon in the cells, which made it easy to collect cells harboring HPV-DNA. The major points are summarized below.

- The HPV replicon has a configuration of plasmid DNA, not of genomic DNA. In previous reports, the genomic-type of DNA was used as a replicon. To obtain the genomic-structure of DNA, full-length HPV-DNA was excised from a plasmid and circularized by self-ligation.[13] This process is laborious and it is difficult to control the quality of the DNA, which influences the transfection efficiency. The self-ligated DNA has a non-supercoiled configuration, and such a form of DNA might not be an appropriate substrate for gene expression and DNA replication. We incorporated, therefore, the HPV-DNA into a plasmid backbone, which made it easier to control the DNA quality and the constancy of the transfection efficiency was improved.
- In the conventional protocol for obtaining the HFKs harboring HPV-DNA, HFKs were transfected with both the genomic-type of DNA and a plasmid expressing a drug-resistance gene, such as pSV2*neo*.[13] After a short period of drug selection, the cells were then expanded without drug selection. The HPV replicon used in this report contained a selection marker, an expression unit for a neomycin-resistance gene, which made it possible to apply the drug-selection even in the expansion process, ensuring that the obtained cells maintained HPV replicons.

In addition to these points, it is unique that p18FLneo contains the LCR at both sides of the genome (Fig. 1). Although we designed it by taking into account the roles of the LCR as 5′- and 3′-regulatory elements, the artificial structure might have unexpected effects on HPV replication. It is necessary, therefore, to compare carefully the replication potentials between the genomic-type DNA and p18FLneo. We also need to determine whether the 3′-LCR unit is required for the maintenance or vegetative replication of HPV-DNA.

Recently Wang *et al.* reported a new system for analyzing the HPV18 lifecycle.[19] They used a plasmid containing HPV18 genome into which a neo^R expression unit and loxP sites were inserted. The plasmid was co-transfected into human keratinocytes along with an expression plasmid for a Nuclear Localization Signal (NLS)-tagged Cre recombinase, resulting in efficient establishment of the cells maintaining almost authentic HPV18 genomic DNA. The most important improvement seemed that they used plasmid DNA instead of the self-ligated genomic-type DNA that did not have a supercoiled structure. The system described in this paper employed a plasmid DNA, p18FLneo, as a replicon, suggesting it has the similar advantage. The long-term selection under the G418 presence is able to be adapted in the system with p18FLneo, but not in the system reported by Wang *et al.* Although their system could produce very high titer of infectious virus, what made this improvement was unexplained, as commented in a review.[32] It will be necessary to perform side-by-side comparison between the systems using p18FLneo and the plasmids used by Wang *et al.*

Usefulness of the new system supporting efficient HPV replication. The new HPV replicon could be maintained stably in HFKs as shown in Figure 2. When applied in the raft culture, the HFKs maintaining the replicon showed moderate hyperplasia and the HPV-DNA was amplified at the differentiated layer of epidermis (Fig. 3). The hyperplasia observed with the raft culture was moderate as compared with that induced by high-risk type E7 expression.[16] The immunoblot analysis of p53 and pRb expressions in the HFKs indicated that the introduction of the HPV replicon suppressed moderately those expressions, suggesting the E6 and E7 expression levels in the HFKs were maintained at low level. It is supposed that the expressions of E6 and E7 are up-regulated in the course of malignant conversion of the HPV-infected cells,[33] thus, the raft culture harboring the HPV replicon seems to represent an early stage of the tumor induced by the HPV infection.

Effects of cytokines in protection against virus infection. Living organisms have protection systems for the viral infections. In mammals, a variety of cytokines are produced by either infected cells or periphery cells, which act in the elimination of the infected cells.[34] The system using the new HPV replicon and the raft culture could be used to examine the effect of cytokine treatment on the early stage of HPV-infected lesions. We selected three cytokines, IFNβ, TNFα, and TGFβ, because there were several reports indicating the relation between these cytokines and HPV infection.[24–30,35,36]

We first examined the effects of the cytokines on the monolayer culture of the HFKs harboring the HPV replicon, which represented the status of the HPV-infected basal cells. Under this condition, although IFNβ treatment could suppress HPV-DNA replication moderately, the treatments of other cytokines, TGFβ and TNFα, had almost no effect on both HPV-DNA replication and cell proliferation (Figs 4,5). HFKs harboring the 18FLneo under the monolayer culture condition showed little signature of viral infection, and the cytokine treatments examined here might not display their effect on such cells. On the contrary, it has been reported that these cytokines have suppressive effects on the growth of HPV-positive cell lines.[24–27,35,36] The cells used in those reports have malignant or transformed phenotype, which might have cause observations different from ours.

Next, the effects were examined using the raft culture (Fig. 6). Under this condition, IFNβ exhibited strong inhibitory effects on dysplasia formation. It also suppressed the vegetative replication of the virus in the suprabasal layer of epithelium. TGFβ also exhibited a significant inhibitory effect on both dysplasia formation and HPV-DNA amplification, but the effect was not as drastic as that of IFNβ. In contrast, it appeared that TNFα treatment enhanced HPV replication and induced the invasion of epithelial cells into the dermal layer.

IFNβ has been administered to HPV-infected lesions including condylomas and early stage cervical intraepithelial neoplasia [23] By using this model, it was possible to confirm the effectiveness of IFNβ on the treatment of HPV-related lesions under tissue culture condition, indicating that this system is a useful platform for examination of the detailed action-mechanisms of IFNβ on HPV replication. Recently, it was reported that p56, a product of ISG56, interacted with viral replication factor E1 and inhibited its function.[37] It will be interesting to examine the induction level of p56 by IFNβ treatment in both the monolayer and raft cultures.

It should be noted that the expressions of E6 and E7 are usually up-regulated in the advanced stages of cervical neoplasia, and they were reported to interfere with the IFN-related pathway by interacting with Tyk2,[38] IRF3,[39] IRF1,[40] or IRF9.[41] Although this report described the significant anti-HPV effects of IFNβ, such effects might be diminished in association with the progression of malignant status.

The observation that TNFα treatment enhanced HPV replication suggests that the inflammatory response accompanied by TNFα production exerts effects opposite to the antiviral response at the early stage of HPV-infected lesions. In searching for new therapeutic approaches to HPV-related diseases, it might be important to consider the induction of inflammation, which has the potential to accelerate disease progression.

In this report, we developed a new experimental system that could support the replication of HPV-DNA for a long period

© 2009 Japanese Cancer Association

and the differentiation-dependent lifecycle of the virus. This system will be adapted to screening for other anti-HPV compounds. It also allows the manipulation of the genetic elements of both host cells and virus; thus, the analysis of regulatory mechanisms of the virus lifecycle and virus-induced tumorigenesis becomes accessible.

Acknowledgments

We thank the many colleagues for technical assistance and manuscript preparation, K. Sasaki for essential advice and support, Dr. P.M. Howley for providing full-length clones for HPV18, and Dr. M. Tsunenaga and Dr. T. Kuroki for instructions regarding the organotypic raft culture. This work is supported in part by a Grant-in-Aid from the Ministry of Health, Labor and Welfare of Japan for the Third-Term Comprehensive 10-year Strategy for Cancer Control. A.S., S.Y., N.K., and H.N. were supported by the 21st Century COE program of the Japan Society for the Promotion of Science (JSPS).

References

1 Howley PM, Lowy DR. Papillomavirus and their replication. In: Knipe DM, Howley PM, eds. *Fields Virology*, 5th edn. Hagerstown: Lippincott Williams & Wilkins,a Wolters Kluwer Business, 2007; 2299–354.
2 Durst M, Gissmann L, Ikenberg H, Zur Hausen H. A papillomavirus DNA from a cervical carcinoma and its prevalence in cancer biopsy samples from different geographic regions. *Proc Natl Acad Sci U S A* 1983; **80**: 3812–5.
3 Zur Hausen H. Papillomavirus infections–a major cause of human cancers. *Biochim Biophys Acta* 1996; **1288**: F55–78.
4 Castellsagué X, De Sanjosé S, Aguado T *et al.* HPV and cervical cancer in the 2007 report. *Vaccine* 2007; **25** (Suppl 3): C1–230.
5 Longworth MS, Laimins LA. Pathogenesis of human papillomaviruses in differentiating epithelia. *Microbiol Mol Biol Rev* 2004; **68**: 362–72.
6 Flores ER, Lambert PF. Evidence for a switch in the mode of human papillomavirus type 16 DNA replication during the viral life cycle. *J Virol* 1997; **71**: 7167–79.
7 Adams JC, Watt FM. Fibronectin inhibits the terminal differentiation of human keratinocytes. *Nature* 1989; **340**: 307–9.
8 Ruesch MN, Laimins LA. Human papillomavirus oncoproteins alter differentiation-dependent cell cycle exit on suspension in semisolid medium. *Virol* 1998; **250**: 19–29.
9 Meyers C, Frattini MG, Hudson JB, Laimins LA. Biosynthesis of human papillomavirus from a continuous cell line upon epithelial differentiation. *Science* 1992; **257**: 971–3.
10 Dollard SC, Wilson JL, Demeter LM *et al.* Production of human papillomavirus and modulation of the infectious program in epithelial raft cultures. *OFF Genes Dev* 1992; **6**: 1131–42.
11 Frattini MG, Lim HB, Laimins LA. In vitro synthesis of oncogenic human papillomaviruses requires episomal genomes for differentiation-dependent late expression. *Proc Natl Acad Sci U S A* 1996; **93**: 3062–7.
12 Moody CA, Fradet-Turcotte A, Archambault J, Laimins LA. Human papillomaviruses activate caspases upon epithelial differentiation to induce viral genome amplification. *Proc Natl Acad Sci U S A* 2007; **104**: 19541–6.
13 Frattini MG, Lim HB, Doorbar J, Laimins LA. Induction of human papillomavirus type 18 late gene expression and genomic amplification in organotypic cultures from transfected DNA templates. *J Virol* 1997; **71**: 7068–72.
14 Strauss WM. Preparation of genomic DNA from mammalian tissue. In: Ausubel FM, Brent R, Kingston RE *et al.*, eds. *Current Protocols in Molecular Biology*. New York: John Wiley & Sons, Inc., 1998; 2.1–2.3.
15 Yoshida S, Kajitani N, Satsuka A, Nakamura H, Sakai H. Ras modifies proliferation and invasiveness of cells expressing human papillomavirus oncoproteins. *J Virol* 2008; **82**: 8820–7.
16 Ueno T, Sasaki K, Yoshida S *et al.* Molecular mechanisms of hyperplasia induction by human papillomavirus E7. *Oncogene* 2006; **25**: 4155–64.
17 Tsunenaga M, Kohno Y, Horii I *et al.* Growth and differentiation properties of normal and transformed human keratinocytes in organotypic culture. *Jpn J Cancer Res* 1994; **85**: 238–44.
18 Sambrool J, Fritsch EF, Maniatis T. *Molecular Cloning*. New York: Cold Spring Harbor Laboratory Press, 1989; 18.30–3.
19 Wang HK, Duffy AA, Broker TR, Chow LT. Robust production and passaging of infectious HPV in squamous epithelium of primary human keratinocytes. *Genes Dev* 2009; **23**: 181–94.
20 Allen-Hoffmann BL, Schlosser SJ, Ivarie CA, Sattler CA, Meisner LF, O'Connor SL. Normal growth and differentiation in a spontaneously immortalized near-diploid human keratinocyte cell line, NIKS. *J Invest Dermatol* 2000; **114**: 444–55.
21 Flores ER, Allen-Hoffmann BL, Lee D, Sattler CA, Lambert PF. Establishment of the human papillomavirus type 16 (HPV-16) life cycle in an immortalized human foreskin keratinocyte cell line. *Virol* 1999; **262**: 344–54.
22 Flores ER, Allen-Hoffmann BL, Lee D, Lambert PF. The human papillomavirus type 16 E7 oncogene is required for the productive stage of the viral life cycle. *J Virol* 2000; **74**: 6622–31.
23 Frazer IH, McMillan NAJ. Papillomatosis and condylomata acuminata. In: Penny S-HaRW, ed. *Clinical Applications of the Interferons*. London: Chapman and Hall Medical, 1997; 79–91.
24 Donalisio M, Cornaglia M, Landolfo S, Lembo D. TGF-beta1 and IL-4 downregulate human papillomavirus-16 oncogene expression but have differential effects on the malignant phenotype of cervical carcinoma cells. *Virus Res* 2008; **132**: 253–6.
25 Nindl I, Steenbergen RD, Schurek JO, Meijer CJ, Van der Valk P, Snijders PJ. Assessment of TGF-beta1-mediated growth inhibition of HPV-16- and HPV-18-transfected foreskin keratinocytes during and following immortalization. *Arch Dermatol Res* 2003; **295**: 297–304.
26 Villa LL, Vieira KB, Pei XF, Schlegel R. Differential effect of tumor necrosis factor on proliferation of primary human keratinocytes and cell lines containing human papillomavirus types 16 and 18. *Mol Carcinog* 1992; **6**: 5–9.
27 Vieira KB, Goldstein DJ, Villa LL. Tumor necrosis factor alpha interferes with the cell cycle of normal and papillomavirus-immortalized human keratinocytes. *Cancer Res* 1996; **56**: 2452–7.
28 Woodworth CD, McMullin E, Iglesias M, Plowman GD. Interleukin 1 alpha and tumor necrosis factor alpha stimulate autocrine amphiregulin expression and proliferation of human papillomavirus-immortalized and carcinoma-derived cervical epithelial cells. *Proc Natl Acad Sci U S A* 1995; **92**: 2840–4.
29 Kyo S, Inoue M, Hayasaka N *et al.* Regulation of early gene expression of human papillomavirus type 16 by inflammatory cytokines. *Virol* 1994; **200**: 130–9.
30 Zur Hausen H. Immortalization of human cells and their malignant conversion by high risk human papillomavirus genotypes. *Semin Cancer Biol* 1999; **9**: 405–11.
31 Dong W, Kloz U, Accardi R *et al.* Skin hyperproliferation and susceptibility to chemical carcinogenesis in transgenic mice expressing E6 and E7 of human papillomavirus type 38. *J Virol* 2005; **79**: 14899–908.
32 Galloway DA. Human papillomaviruses: a growing field. *Genes Dev* 2009; **23**: 138–42.
33 Munger K, Howley PM. Human papillomavirus immortalization and transformation functions. *Virus Res* 2002; **89**: 213–28.
34 Takeuchi O, Akira S. Recognition of viruses by innate immunity. *Immunol Rev* 2007; **220**: 214–24.
35 Stanley MA, Pett MR, Coleman N. HPV: from infection to cancer. *Biochem Soc Trans* 2007; **35**: 1456–60.
36 Koromilas AE, Li S, Matlashewski G. Control of interferon signaling in human papillomavirus infection. *Cytokine Growth Factor Rev* 2001; **12**: 157–70.
37 Terenzi F, Saikia P, Sen GC. Interferon-inducible protein, P56, inhibits HPV DNA replication by binding to the viral protein E1. *EMBO J* 2008; **27**: 3311–21.
38 Li S, Labrecque S, Gauzzi MC *et al.* The human papilloma virus (HPV)-18 E6 oncoprotein physically associates with Tyk2 and impairs Jak-STAT activation by interferon-alpha. *Oncogene* 1999; **18**: 5727–37.
39 Ronco LV, Karpova AY, Vidal M, Howley PM. Human papillomavirus 16 E6 oncoprotein binds to interferon regulatory factor-3 and inhibits its transcriptional activity. *Genes Dev* 1998; **12**: 2061–72.
40 Perea SE, Massimi P, Banks L. Human papillomavirus type 16 E7 impairs the activation of the interferon regulatory factor-1. *Int J Mol Med* 2000; **5**: 661–6.
41 Antonsson A, Payne E, Hengst K, McMillan NA. The human papillomavirus type 16 E7 protein binds human interferon regulatory factor-9 via a novel PEST domain required for transformation. *J Interferon Cytokine Res* 2006; **26**: 455–61.

doi: 10.1111/j.1349-7006.2009.01411.x
© 2009 Japanese Cancer Association

Virology 406 (2010) 181–188

Contents lists available at ScienceDirect

Virology

journal homepage: www.elsevier.com/locate/yviro

Inhibition of nuclear entry of HPV16 pseudovirus-packaged DNA by an anti-HPV16 L2 neutralizing antibody

Yoshiyuki Ishii [a,*], Keiko Tanaka [b], Kazunari Kondo [c], Takamasa Takeuchi [a], Seiichiro Mori [a], Tadahito Kanda [a]

[a] Pathogen Genomics Center, National Institute of Infectious Diseases, 1-23-1 Toyama, Shinjuku-ku, Tokyo 162-8640, Japan
[b] Department of Pathology, National Institute of Infectious Diseases, 1-23-1 Toyama, Shinjuku-ku, Tokyo 162-8640, Japan
[c] Department of Gynecology and Obstetrics, NTT Medical Center Tokyo, 5-9-22, Higashi-Gotanda, Shinagawa-Ku, Tokyo, 141-8625, Japan

ARTICLE INFO

Article history:
Received 1 April 2010
Returned to author for revision 13 May 2010
Accepted 9 July 2010
Available online 4 August 2010

Keywords:
HPV16
L2
Neutralizing antibody
Anti-P56/75

ABSTRACT

Rabbit anti-HPV16 L2 serum (anti-P56/75) neutralizes multiple oncogenic human papillomaviruses (HPVs). We inoculated HeLa cells with HPV16 pseudovirus (16PV) and with anti-P56/75-bound 16PV (16PV-Ab). Both 16PV and 16PV-Ab attached equally well to the cell surface. However, the cell-attached L1 protein of 16PV became trypsin-resistant after incubation at 37 °C, whereas approximately 20% of the cell-attached 16PV-Ab L1 remained trypsin-sensitive. Confocal microscopy of HeLa cells inoculated with 16PV revealed packaged DNA in the nucleus at 22 h after inoculation; however, nuclear DNA was not detected in cells inoculated with 16PV-Ab. Electron microscopy of HeLa cells inoculated with 16PV showed particles located in multivesicular bodies, lamellar bodies, and the cytosol after 4 h; no cytosolic particles were detected after inoculation with 16PV-Ab. These data suggest that anti-P56/75 inhibits HPV infection partly by blocking viral entry and primarily by blocking the transport of the viral genome to the nucleus.

© 2010 Elsevier Inc. All rights reserved.

Introduction

Human papillomavirus (HPV) consists of a double-stranded DNA genome (8 kb) and a non-enveloped icosahedral capsid composed of two capsid proteins, L1 (major) and L2 (minor) (Howley and Lowy, 2001). Based on nucleotide similarities among their L1 genes, HPVs have been classified into more than 100 genotypes. HPV genotype 16 (HPV16) is the most prevalent type linked to cervical cancer worldwide.

HPV propagates only in differentiating keratinocytes (zur Hausen, 2002), which are difficult to culture on a large scale. Hence, it is difficult to prepare HPV virions for detailed studies of the HPV infection process. As a surrogate virus, an infectious HPV pseudovirus, comprising an HPV capsid containing a reporter plasmid, has been developed (Buck et al., 2004). When SV40 T-antigen-positive cells are transfected with expression plasmids for L1 and L2 together with a reporter plasmid carrying SV40-ori, the replicating reporter plasmid is packaged into the capsid formed by the assembly of L1 and L2 in the nucleus, thereby producing pseudovirus (PV). Human cells inoculated with PV express a readily detectable level of the reporter.

Thus far, many studies with PVs have indicated that PV binds to heparin sulfate proteoglycans (HSPGs) on the surface of cells (Giroglou et al., 2001) and then enters the cells by endocytosis mediated by clathrin, caveolin, or the tetraspanin microdomain region (Bousarghin et al., 2003; Day et al., 2003; Hindmarsh and Laimins, 2007; Smith et al., 2008; Spoden et al., 2008). The vesicles containing PV traffic to endosomal compartments, including late endosomes, lysosomes, and cavoesomes (Day et al., 2003; Smith et al., 2008). The mechanisms of viral egress from the organelles and viral uncoating are not clear, but it has been suggested that the minor capsid protein, L2, plays an important role in these events (Day et al., 2004; Kämper et al., 2006; Richards et al., 2006).

L2 is composed of about 470 amino acids. The C-terminal region of L2 binds to L1 (Okun et al., 2001; Finnen et al., 2003). The N-terminal region, with an amino acid sequence that is highly conserved among various HPV types, contains several cross-neutralization epitopes (Pastrana et al., 2005; Kondo et al., 2007). Antiserum obtained from rabbits immunized with a synthetic peptide representing the sequence of HPV16 amino acid residues 56 to 75 (anti-P56/75) neutralizes genotype 16, 18, 31, and 58 PVs (Kondo et al., 2007), as 7well as HPV16 authentic virions produced by raft culture (Conway et al., 2009).

In the present study, we incubated HPV16 PV (16PV) with anti-P56/75 serum or normal rabbit serum and used this to inoculate HeLa cells. We examined the inoculated cells for 16PV attachment to the

* Corresponding author. Fax: +81 3 5285 1166.
E-mail address: yishii@nih.go.jp (Y. Ishii).

0042-6822/$ – see front matter © 2010 Elsevier Inc. All rights reserved.
doi:10.1016/j.virol.2010.07.019

cell surface, internalization of 16PV, and the intracellular localization of 16PV particles and DNA. The results showed that approximately 20% of the antibody-bound 16PV particles failed to enter the cell, and the internalized antibody-bound 16PV particles failed to transport the packaged DNA to the nucleus.

Results

Neutralization of 16PV by anti-P56/75

To examine the effect of anti-P56/75 on pseudoviral infection, HeLa cells were inoculated with 16PV (2.5 μg) preincubated with normal rabbit serum or 16PV (2.5 μg) preincubated with anti-P56/75 serum. After 2 days in culture, cells positive for EGFP were identified by fluorescence microscopy (Fig. 1A) and were counted by fluorescence-activated cell sorting (FACS) (Fig. 1B). Cells inoculated with 16PV preincubated with normal rabbit serum efficiently expressed EGFP (Fig. 1A, upper panel), whereas cells inoculated with 16PV preincubated with anti-P56/75 (1:20 dilution) did not express the reporter protein (Fig. 1A, lower panel). A FACS analysis of 10,000 cells inoculated with 16PV preincubated with normal rabbit serum revealed 6000 EGFP-positive cells (Fig. 1B). In contrast, cells inoculated with 16PV preincubated with anti-P56/75 serum (1:20 dilution) showed almost no EGFP expression by FACS analysis. These data indicate that the incubation of 16PV with anti-P56/75 serum prevented the expression of the PV reporter protein in inoculated cells.

Effect of anti-P56/75 on 16PV attachment to and entry into HeLa cells

To determine the effect of anti-P56/75 on the attachment of 16PV to the cell surface, HeLa cells were incubated with 16PV preincubated with normal rabbit serum or 16PV preincubated with anti-P56/75 serum for 1 h at 4 °C, harvested, lysed, and analyzed by Western blotting with anti-HPV16 L1 monoclonal antibody (Fig. 2A). The antibody recognized similar levels of the L1 virus protein in both cell samples, indicating that the binding of anti-P56/75 to 16PV did not block the attachment of 16PV to the cells.

To investigate the effect of anti-P56/75 on the entry of the virus into cells, HeLa cells inoculated with 16PV preincubated with normal rabbit serum or 16PV preincubated with anti-P56/75 serum were incubated at 37 °C for the indicated times and harvested in the presence or absence of trypsin. After being washed, the cells were lysed and analyzed for the presence of L1 by Western blotting with anti-HPV16 L1 monoclonal antibody (Fig. 2B). In cells without incubation (time 0), L1 was not present in the lysates of cells harvested with trypsin, indicating that L1 had been separated from the cells and digested by trypsin (Supplementary Fig. 1A). Thus, 16PV was still on the surface of the cells before incubation at 37 °C. After 2 h of incubation, some L1 was not digested by trypsin during harvesting

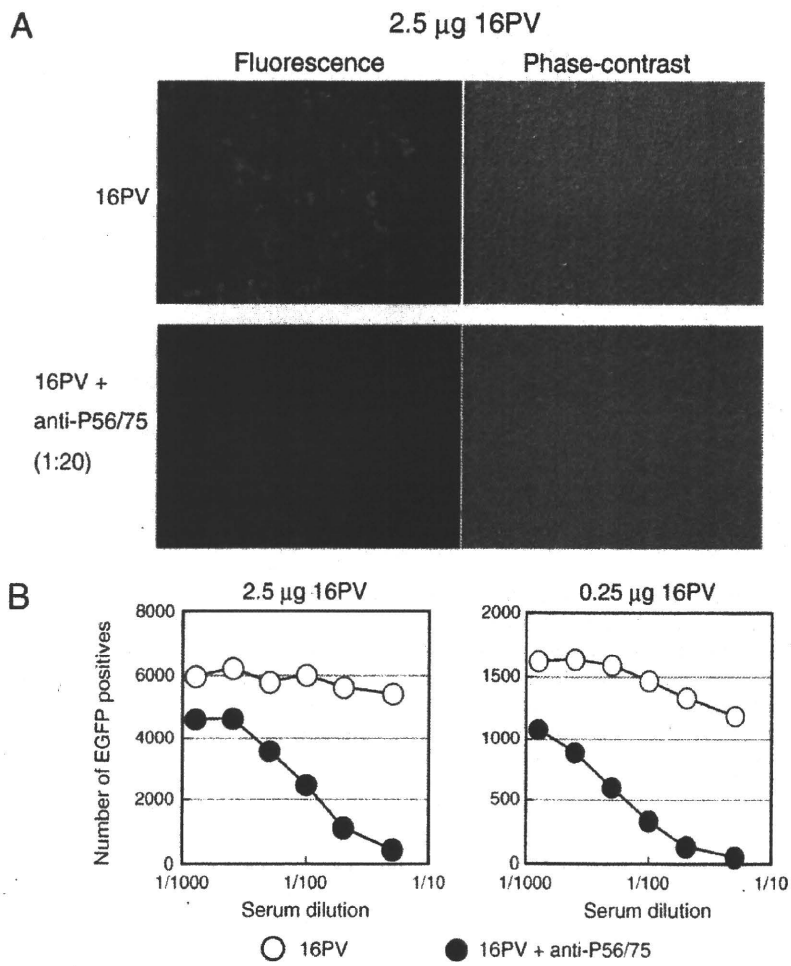

Fig. 1. Neutralization of 16PV by anti-P56/75. The pseudovirus 16PV (2.5 μg or 0.25 μg of L1, as indicated), which carries an expression plasmid for EGFP, was mixed with anti-P56/75 serum or normal rabbit serum in growth medium (500 μl) and incubated at 37 °C for 30 min. HeLa cells were inoculated with the mixture and incubated. After 2 days, the EGFP signal of the cells was observed by fluorescence microscopy (A), and the number of EGFP-positive cells among 10^4 cells was counted by fluorescence-activated cell sorting (FACS) (B). The experiments were performed in duplicate.

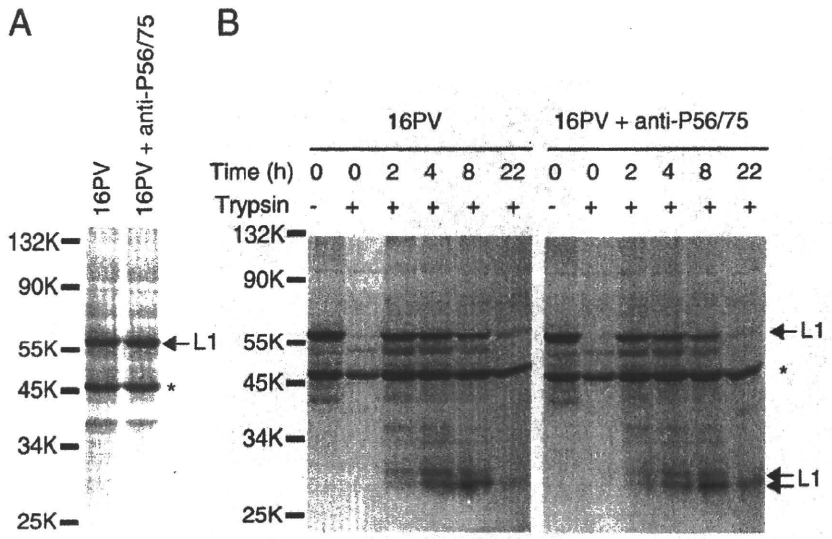

Fig. 2. Attachment and entry of 16PV to HeLa cells. (A) Attachment of 16PV to cells. The 16PV (2.5 μg of L1) was mixed with anti-P56/75 serum or normal rabbit serum (final dilution, 1:20) in growth medium (500 μl) and incubated at 37 °C for 30 min. HeLa cells were inoculated with the mixture and incubated at 4 °C for 1 h. The cells were washed with cold PBS, harvested in PBS containing 2.5 mM EDTA, and then lysed. L1 protein in the lysate was detected by Western blotting with mouse anti-HPV16 L1 antibody. Experiments were performed independently in triplicate. (B) Trypsin resistance of L1. Cells were inoculated and incubated at 4 °C for 1 h as described above. The cells were washed with growth medium and incubated in growth medium at 37 °C for 0, 2, 4, 8, and 22 h. At each time point, the cells were harvested in PBS containing 2.5 mM EDTA (trypsin−) or trypsin (trypsin +) and then lysed. L1 protein in the lysate was detected by Western blotting with mouse anti-HPV16 L1 antibody. Arrows indicate full-sized and degraded L1. Asterisks indicate an unknown protein that reacted with the antibody. Experiments were performed independently in triplicate.

and appeared in the cell lysates, indicating that 16PV had entered the cells. Degraded, smaller L1 fragments appeared in cell lysates at 2 h and became prominent at 4 h. The levels of both intact and degraded L1 were reduced at 22 h, suggesting that L1 was further degraded. The levels of trypsin-resistant L1 in the lysates of cells inoculated with anti-P56/75-bound 16PV (right panel) were approximately 80% of those in lysates of cells inoculated with 16PV in the absence of anti-P56/75 (left panel and Table 1). Thus, approximately 20% of the cell-attached antibody-bound PV failed to enter the cells.

The cells that internalized 16PV in the absence of anti-P56/75 showed reporter protein expression at 2, 4, and 8 h of incubation following inoculation (Supplementary Fig. 1B), indicating that the internalized 16PV was delivered through the infectious pathway.

Effect of anti-P56/75 on the subcellular localization of 16PV L1 and packaged DNA in HeLa cells

To examine the subcellular localizations of 16PV L1 and the DNA packaged inside the capsid, the DNA was labeled by replacing thymidine with 5-ethynil-2′-deoxyuridine (EdU) during replication. EdU-labeled DNA in 16PV lost the ability to express the reporter gene in inoculated 293FT cells (Supplementary Fig. 2). HeLa cells were inoculated with EdU-labeled 16PV preincubated with normal rabbit serum or preincubated with anti-P56/75 serum. The cells were then incubated at 37 °C for the indicated times, fixed with methanol, and fluorescently stained for L1 (Alexa Fluor 555, red signal) and EdU-labeled DNA (Alexa Fluor 488, green signal). Where L1 and the DNA colocalized, the overlapping signals appeared as yellow dots (Fig. 3).

Confocal fluorescence microscopy images show the intracellular localization of L1 and EdU-DNA in HeLa cells inoculated with 16PV preincubated with normal rabbit serum (Fig. 3A, left panel) and in HeLa cells inoculated with 16PV preincubated with anti-P56/75 serum (Fig. 3A, right panel). In each panel, differential interference contrast images are presented to the right of the fluorescence images. The numbers of red, green, and yellow dots at different incubation times are given in Fig. 3B.

In cells inoculated with EdU-labeled PV16 preincubated with normal rabbit serum (Fig. 3A, left panel), capsids with EdU-labeled DNA (yellow dots) and empty capsids or capsids with unlabeled DNA (red dots) were located along the surface of the cells, at a ratio of about 3:2, respectively, before incubation at 37 °C (time 0 h). After incubation at 37 °C for 2 h, some yellow and red dots appeared in the cytoplasm, representing internalization of 16PV. Between 4 and 8 h of incubation, the number of yellow and red dots in the cytoplasm decreased (Fig. 3B). At 22 h, several green dots (approximately 6 ± 3 dots/cell), indicating EdU-labeled DNA that had separated from the capsid, appeared in the nucleus, and some small red dots, representing L1, were seen in the perinuclear region (Figs. 3A and B). Thus, the packaged DNA was released from the capsid and entered the nucleus during incubation at 37 °C.

In cells inoculated with EdU-labeled 16PV preincubated with anti-P56/75 serum, many yellow and red dots were located along the cell surface at time 0 (Fig. 3A, right panel). At 2 h, large yellow dots, which were probably aggregates of 16PV, appeared on the cell surface, where they remained until 22 h. At 22 h, red dots were observed in the perinuclear region, but no green dots were ever present in the nucleus (Figs. 3A and B).

Table 1
Percentage of trypsin-resistant L1[a].

	Incubation at 37 °C	
	2 h	4 h
16 V	64.3 (16.5)	64.9 (3.71)
16 V + anti-P56/75	52.1 (17.1)	53.9 (9.13)

Results are presented as average percentage of three independent experiments (standard deviation).
[a] Cell-attached L1 at 0 h was set to 100%.

Effect of anti-P56/75 on the subcellular localization of 16PV particles in HeLa cells

The subcellular localization of 16PV particles in HeLa cells was studied using transmission electron microscopy (Fig. 4). HeLa cells were inoculated with 16PV preincubated with normal rabbit serum or

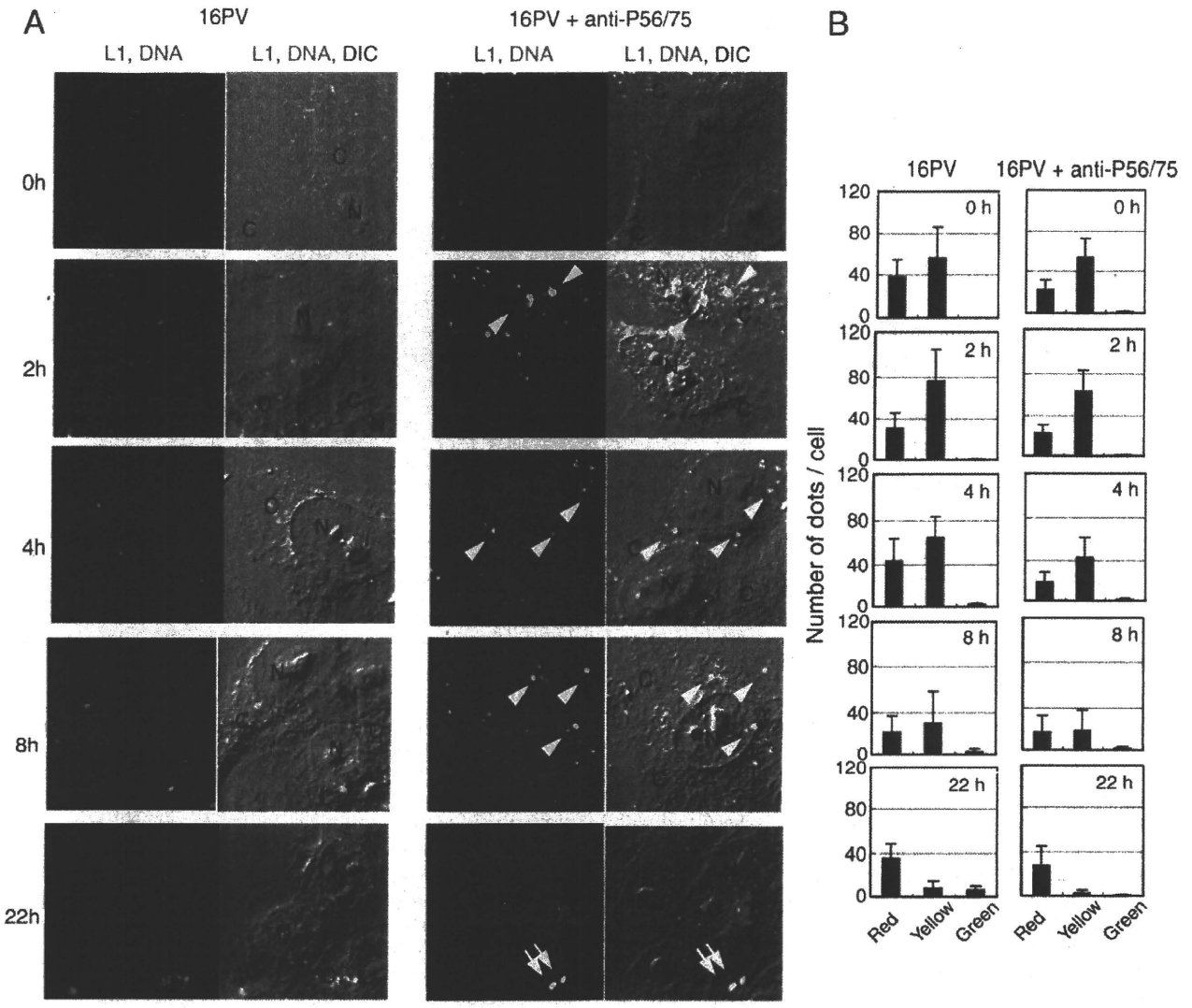

Fig. 3. Subcellular localization of L1 protein and packaged DNA. (A) The 16PV (2.5 μg of L1) containing 5-ethynil-2′-deoxyuridine (EdU)-labeled DNA was preincubated with anti-P56/75 serum (final dilution, 1:20) or normal rabbit serum in growth medium (500 μl) at 37 °C for 30 min and used to inoculate HeLa cells. The cells were incubated at 4 °C for 1 h, washed with growth medium, incubated in growth medium at 37 °C for 0, 2, 4, 8, and 22 h, fixed with methanol, and fluorescently labeled for L1 (Alexa Fluor 555, red dots) and EdU-labeled DNA (Alexa Fluor 488, green dots). Colocalized L1 and DNA appear as yellow dots. Confocal fluorescence microscopy images of cells inoculated with 16PV in the absence (left panel) and presence of anti-PV56/75 (right panel) are presented, along with the differential interference contrast images. The small arrowheads indicate a large aggregate of antibody-bound 16PV particles, thought to be on the cell surface. The arrows indicate an aggregate that appears to be at the contact site between two adjacent cells. Experiments were performed twice independently. N: nucleus, C: cytoplasm. (B) Numbers of red, yellow, and green dots in the cells. Red (L1), yellow (L1 and DNA), and green (DNA) dots were counted in 20 randomly selected cells of the indicated samples. Error bars represent the standard deviation.

16PV preincubated with anti-P56/75 serum. HeLa cells in the absence of 16PV served as a control. After a 4-h incubation, the cells were fixed and embedded. Ultra-thin sections (70 nm) were cut, stained with 4% uranyl acetate, and viewed under a transmission electron microscope.

HeLa cells incubated with either 16PV preparation showed particles with an approximate diameter of 55 nm on their surface (Figs. 4B and C). The electron-dense particles were probably capsids containing DNA, as these particles were not detected on the cells incubated without 16PV (Figs. 4A and E). The particles of antibody-bound 16PV formed a large aggregate (Fig. 4C), but no particle aggregation was detected in the cells inoculated with 16PV in the absence of antibody (Fig. 4B). This result is consistent with the confocal microscopy images of the cells at 2 and 4 h. The aggregate was likely unable to enter the cell and remained on the cell surface.

The particles of 16PV were located in multivesicular bodies (MVBs; 200–500 nm and 500–1,000 nm in diameter), which are late endosomes containing multiple lumenal vesicles; in lamellar bodies (LBs), which are lysosomal organelles containing multiple concentric membrane layers (Schmitz and Müller, 1991); in lysosome-like MVBs (L-MVBs), which are relatively electron-dense organelles; and in the cytosol (Figs. 4D and F, capsids are indicated by arrows). There were fewer particles of antibody-bound 16PV, and these were located in MVBs and L-MVBs, but not in the large MVBs (500–1000 nm in diameter) or the cytosol (Table 2). Some 16PV particles were attached to the limiting membrane of MVBs (Fig. 4F), whereas no particles of antibody-bound 16PV were attached to the membrane (Fig. 4G). These observations suggest that any antibody-bound 16PV that entered the cell did not egress from the endosomal compartments.

Discussion

In the present study, the binding of anti-P56/75 to 16PV did not affect the attachment of 16PV to HeLa cells, as shown by Western blot analysis of cell lysates and by confocal fluorescence microscopy. In

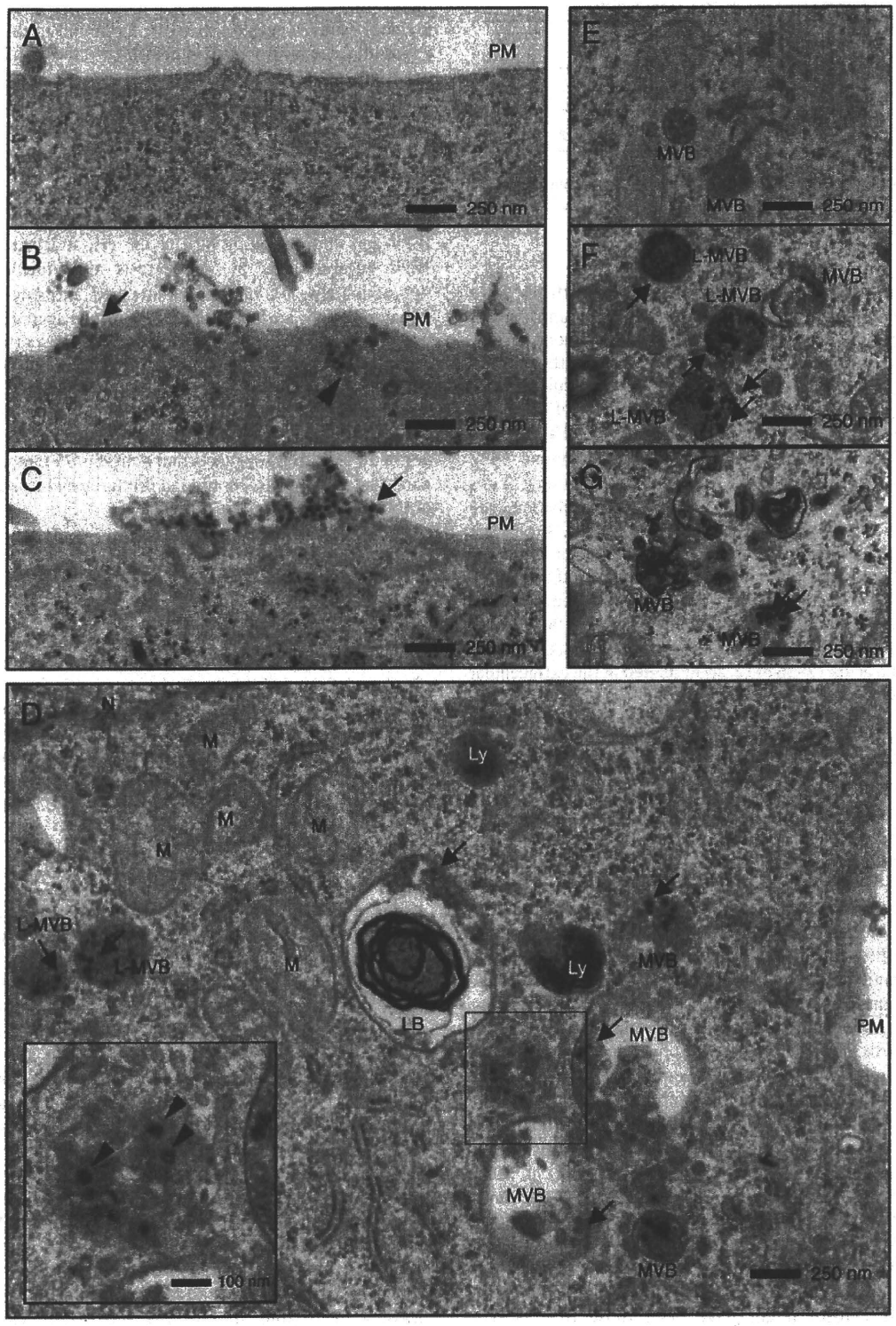

Fig. 4. Subcellular localization of 16PV particles. The 16PV (10 μg of L1) was mixed with anti-P56/75 serum or normal rabbit serum (final dilution, 1:10) in growth medium (1 ml) and incubated at 37 °C for 30 min. HeLa cells (6×10^5) were inoculated with the mixture, incubated at 37 °C for 4 h, fixed, and embedded. Ultra-thin sections were cut and stained with uranyl acetate for observation by transmission electron microscopy. A and E: Cells were not inoculated with 16PV. B, D, and F: Cells were inoculated with 16PV preincubated with normal rabbit serum. C and G: Cells were inoculated with 16PV preincubated with anti-P56/75 serum. Arrows in B and C indicate particles on the cell surface. The arrowhead in B indicates an invagination of the plasma membrane. The arrows in D indicate particles in endosomal compartments (MVBs, LBs, and L-MVBs); cytosolic particles are boxed, and an enlargement is shown in the inset. The arrows in F indicate particles located near the limiting membranes of L-MVBs. The arrow in G indicates particles in MVBs. Experiments were performed twice independently. LB: lamellar body; L-MVB: lysosome-like multiple vesicular body; Ly: lysosome; M: mitochondrion; MVB: multiple vesicular body; N: nucleus; PM: plasma membrane.

Table 2
Intracellular distribution of electron-dense particles with an approximate diameter of 55 nm at 4 h post-inoculation.

	Number of 55-nm electron-dense particles[a]									
	Cell surface		LBs		MVBs		L-MVBs		Cytosol	
	#1	#2	#1	#2	#1	#2	#1	#2	#1	#2
16PV	27	140	2.5	0.4	13	19	12	15	1.8	1.4
16PV + anti-P56/75	28	110	0	0	7	1.4	4.3	0.8	0	0

Experiments were performed twice independently.
[a] The number of particles is shown as the average from five cells photographed at a magnification of ×20,000.

both the presence and absence of antibody, 16PV particles were observed on the surface of inoculated HeLa cells. Thus, anti-P56/75 did not neutralize 16PV by interfering with viral attachment to cells.

The binding of anti-P56/75 to 16PV partially blocked the entry of cell-attached 16PV into HeLa cells. After incubation of inoculated HeLa cells at 37 °C, the trypsin resistance of the L1 protein of antibody-bound 16PV was only 80% of the trypsin resistance of 16PV L1 in the absence of antibody, indicating that 20% of antibody-bound 16PV remained on the cell surface, where it appeared to form aggregates visible by confocal microscopy after 2 to 22 h of incubation. The aggregates were also observed by electron microscopy, suggesting that the aggregates that formed after the attachment of PV to the surface were not degraded and remained for a long period on the cell surface. This indicates that anti-P56/75 did not mediate the formation of large aggregates of virion by acting as a bivalent tether. In a similar previous experiment, 16PV bound with RG-1, a monoclonal antibody recognizing amino acids 17–36 of L2, accumulated in the extracellular matrix contacting the cell edges (Day et al., 2008).

The binding of anti-P56/75 to 16PV blocked the release of the packaged DNA from the internalized PV to the nucleus. On confocal fluorescence micrographs, DNA released from capsids was observed in the nuclei of cells inoculated with 16PV preincubated with normal serum and incubated for 22 h; however, no evidence of released DNA was seen in cells inoculated with antibody-bound 16PV.

Electron micrographs of HeLa cells at 4 h after the inoculation clearly showed that cells inoculated with antibody-bound 16PV contained fewer 16PV particles than cells inoculated with 16PV in the absence of antibody, even though the antibody impaired the internalization efficiency of 16PV by only about 20%. It is possible that the capsids of antibody-bound 16PV were easily denatured in the cells, making some particles undetectable by electron microscopy. Based on the electron micrographs, antibody-bound 16PV entered the cells by endocytosis, but failed to egress from endosomal vesicles. In the absence of antibody, 16PV particles were seen in MVBs, LBs, and the cytosol (Fig. 4C), whereas particles of antibody-bound 16PV were observed in some MVBs, but not in the cytosol. Previous studies have shown that the most BPV1 virions, BPV1 PV, HPV16 capsids, and HPV31 capsids accumulate in endosomal vesicles (Zhou et al., 1995; Bossis et al., 2005; Bousarghin et al., 2003), and a small fraction of inoculated HPV16 capsids or BPV1 PV has been detected in the cytosol (Yang et al., 2003; Bossis et al., 2005). In general, particles in endosomal vesicles are degraded after fusion of the vesicles with lysosomes (Day et al., 2003). In the present study, the particles observed in the cytosol might have been those that escaped degradation.

The structure of particles in the cytosol must be altered in order to release the viral genome from the virion. These dynamic structural changes may be induced by cyclophilin A, a cytosolic peptidyl-prolyl cis/trans isomerase that facilitates 16PV infection (Bienkowska-Haba et al., 2009), and by cell cycle progression through mitosis, which is an important event for HPV infection (Pyeon et al., 2009).

The attachment of particles to the limiting membranes of MVBs, as reported in the present study, may be vital for particles to exit the vesicles, considering that no antibody-bound 16PV particles were found attached to MVB limiting membranes or in the cytosol. A previous study suggested that HPV L2 bound to the lipid bilayer of endosomal compartments and destabilized the membrane, according to a decrease of the internal pH (Kämper et al., 2006); this eventually led to the viral genome entering the nucleus. Anti-P56/75 binds to the L2 region displayed on the surface of HPV pseudovirus (Kondo et al., 2007) and may thereby block an L2 function necessary for binding to and destabilizing the limiting membrane.

In summary, 16PV alone and antibody-bound 16PV showed similar attachment to the surface of HeLa cells. Almost all of the cell-attached 16PV and approximately 80% of the cell-attached antibody-bound 16PV entered cells by endocytosis after incubation at 37 °C. Approximately 20% of the cell-attached antibody-bound particles remained on the surface, where they formed aggregates. A portion of the 16PV particles exited the vesicles and transported the packaged DNA to the nucleus. In contrast, all of the antibody-bound 16PV particles remained in vesicles, to be degraded after the fusion of the vesicles with lysosomes. It is likely that an L2 function essential for egress from vesicles is abrogated by the binding of anti-P56/75 antibody. This study suggests that anti-P56/75 inhibits HPV infection partly by blocking viral entry and primarily by blocking the transport of the viral genome to the nucleus.

Materials and methods

Cells

The 293FT cell line expressing a high level of SV40 T-antigen was purchased from Life Technologies Corp. (Carlsbad, CA, USA). The 293FT and HeLa cells were cultured in Dulbecco's modified Eagle's medium (DMEM) (Life Technologies Corp.) supplemented with 10% fetal bovine serum, 100 units/ml penicillin G potassium (Meiji Seika Ltd., Tokyo, Japan), and 60 μg/ml kanamycin sulfate (Wako Pure Chemical Industries Ltd., Tokyo, Japan) at 37 °C in 5% CO_2.

Production of 16PV

The 16PV consisted of a HPV16 capsid containing a reporter plasmid encoding enhanced green fluorescence protein (pEF1a-EGFP) and was produced as described previously (Ishii et al., 2007; Kondo et al., 2007). To label the 16PV-packaged DNA with 5-ethynil-2′-deoxyuridine (EdU) (Life Technologies Corp.), 293FT cells (1×10^7) were incubated for 16 h in a 10-cm culture dish; transfected with a mixture of p16L1h (13.5 μg), p16L2h (3 μg), and pYSEAP (13.5 μg) (Kondo et al., 2007) by using Fugene HD (Roche Diagnostics GmbH, Mannheim, Germany); incubated for 6 h at 37 °C; and supplemented with 100 μM EdU. After 60 h, the cells were harvested using a cell scraper, suspended in 500 μl of lysis buffer [PBS containing 1 mM $CaCl_2$, 10 mM $MgCl_2$, 0.35% Brij58 (Sigma-Aldrich, St. Louis, MO, USA), 0.1% benzonase (Sigma-Aldrich), 0.1% plasmid-safe ATP-dependent DNase (Epicentre Corp., Madison, WI, USA), and 1 mM ATP], and incubated for 30 h at 37 °C with slow rotation, in the dark. The lysate was cooled on ice for 5 min, mixed with 5 M NaCl to a final NaCl concentration of 1 M, kept on ice for 10 min, and then centrifuged at 5000×*g* for 10 min at 4 °C. The supernatant was placed on an Optiprep (Axis-Shield PoC AS, Oslo, Norway) gradient (from top to bottom, 27%, 33%, and 39% in PBS containing 1 mM $CaCl_2$, 10 mM $MgCl_2$, and 0.85 M NaCl) and centrifuged at 50,000 rpm for 3.5 h at 16 °C in an SW55Ti rotor (Beckman Coulter Inc., Fullerton, CA, USA). Fractions (400 μl each) were obtained by puncturing the bottom of the tube. Aliquots (5 μl per fraction) were analyzed by SDS-PAGE. The fraction in which L1 was most abundant was used as the 16PV stock.

Neutralization assay

The 16PV (0.25 μg or 2.5 μg of L1) was mixed with normal rabbit serum (Life Technologies Corp.) or rabbit anti-P56/75 serum (Kondo et al., 2007), at serial dilutions from 1:20 to 1:800, in 500 μl of growth medium and incubated at 37 °C for 30 min. Each mixture was added to HeLa cells (1.5×10^5) in 24-well plates. After incubation for 2 days, the cells were examined under a BZ-8000 fluorescence microscope (Keyence, Osaka, Japan) and harvested using trypsin. EGFP-positive cells were counted by flow cytometry (FACSCalibur; Becton Dickinson and Co., San Jose, CA, USA).

Western blot assay

The 16PV (2.5 μg of L1) was mixed with normal rabbit serum or rabbit anti-P56/75 serum (1:20 dilution) in 500 μl of growth medium and incubated at 37 °C for 30 min. Each mixture was added to HeLa cells (1.5×10^5) in 24-well plates. The cells were incubated for 1 h at 4 °C, washed with PBS, harvested in PBS containing 2.5 mM EDTA, and lysed. The lysate proteins were separated by SDS-PAGE and transferred to a polyvinylidene difluoride membrane. The L1 protein was detected by immunoblotting with mouse monoclonal anti-HPV16 L1 antibody (BD Biosciences Pharmingen, San Diego, CA, USA), followed by anti-mouse IgG-HRP (Santa Cruz Biotechnology Inc., Santa Cruz, CA, USA). Immunoreactive bands were visualized using an ECL Plus Western blot detection system (GE Healthcare UK Ltd., Little Chalfont, Buckinghamshire, England) and Typhoon 9410 (GE Healthcare UK Ltd.).

Internalization assay

The 16PV (2.5 μg of L1) was mixed with normal rabbit serum or rabbit anti-P56/75 serum (1:20 dilution) in 500 μl of growth medium and incubated at 37 °C for 30 min. Each mixture was added to HeLa cells (1.5×10^5) in 24-well plates. After incubation for 1 h at 4 °C, the cells were washed with PBS, cultured at 37 °C for 0, 2, 4, 8, and 22 h, and harvested with PBS containing trypsin (trypsin+) or containing 2.5 mM EDTA (trypsin−). The cells were lysed and electrophoresed in a SDS-polyacrylamide gel. The separated proteins were transferred to a polyvinylidene difluoride membrane, and a Western blot was performed as described above.

Immunofluorescence assay

The 16PV (2.5 μg of L1) containing EdU-labeled DNA was mixed with normal rabbit serum or rabbit anti-P56/75 serum (1:20 dilution) in 500 μl of growth medium and incubated at 37 °C for 30 min. The mixture was added to HeLa cells (1.5×10^5) in the wells of four-chamber glass slides (BD Biosciences Falcon, Bedford, MA, USA), followed by incubation for 1 h at 4 °C. The cells were washed with growth medium, incubated in growth medium for 0, 2, 4, 8, and 22 h at 37 °C, washed with PBS, and fixed with methanol for 30 min at −20 °C. After washing twice with 3% BSA in PBS for 5 min, the cells were incubated with Click-it Reaction Cocktail containing Alexa Fluor 488 (Click-it™ EdU imaging kit; Life Technologies Corp.) for 30 min at room temperature (RT) in the dark and again washed twice with 3% BSA in PBS for 5 min. Next, the cells were incubated with mouse anti-HPV16 L1 polyclonal antiserum, which had been produced previously by immunizing mice with HPV16 L1 VLP (Ishii et al., 2003), in PBS containing 3% BSA for 1 h at RT and washed with PBS containing 0.2% Tween-20. The cells were then incubated with Alexa Fluor 555-conjugated goat anti-mouse IgG (H+L) (Life Technologies Corp.) in PBS containing 3% BSA, washed with PBS containing 0.2% Tween-20, and mounted with ProLong Gold anti-fade reagent with DAPI (Life Technologies Corp.). Fluorescence was examined using a Fluoview FV1000 confocal microscope (Olympus, Tokyo, Japan).

Electron microscopy

The 16PV (10 μg of L1) was mixed with normal rabbit serum or rabbit anti-P56/75 serum (1:10 dilution) in 1 ml of growth medium and incubated at 37 °C for 30 min. Each mixture was added to HeLa cells (6×10^5) in 35-mm culture plates. After incubation at 37 °C for 1 h, 1 ml of growth medium was added to the cells, and the cells were incubated at 37 °C for another 3 h (4 h total). After incubation, the cells were prefixed in 2.5% glutaraldehyde/0.1 M phosphate buffer at RT for 2 h, washed with phosphate buffer for 30 min, and post-fixed in 1% osmium tetroxide for 1 h. Following dehydration in a graded series of ethanol solutions, the cells were embedded in a mixture of Epoxy 812, DDSA, MNA, and DMP-30 at 60 °C for 2 days. Ultra-thin sections (70 nm) were cut parallel to the substrate, stained with 4% uranyl acetate, and examined under a Hitachi H-7650 transmission electron microscope.

Acknowledgments

This work was supported by a grant-in-aid for the Third-Term Comprehensive 10-year Strategy for Cancer Control from the Ministry of Health, Labour, and Welfare of Japan.

Appendix A. Supplementary data

Supplementary data associated with this article can be found, in the online version, at doi:10.1016/j.virol.2010.07.019.

References

Bienkowska-Haba, M., Patel, H.D., Sapp, M., 2009. Target cell cyclophilins facilitate human papillomavirus type 16 infection. PLoS Pathog. 5, e1000524.
Bossis, I., Roden, R.B., Gambhira, R., Yang, R., Tagaya, M., Howley, P.M., Meneses, P.I., 2005. Interaction of tSNARE syntaxin 18 with the papillomavirus minor capsid protein mediates infection. J. Virol. 79, 6723–6731.
Bousarghin, L., Touzé, A., Sizaret, P.Y., Coursaget, P., 2003. Human papillomavirus types 16, 31, and 58 use different endocytosis pathways to enter cells. J. Virol. 77, 3846–3850.
Buck, C.B., Pastrana, D.V., Lowy, D.R., Schiller, J.T., 2004. Efficient intracellular assembly of papillomaviral vectors. J. Virol. 78, 751–757.
Conway, M.J., Alam, S., Christensen, N.D., Meyers, C., 2009. Overlapping and independent structural roles for human papillomavirus type 16L2 conserved cysteines. Virology 393, 295–303.
Day, P.M., Lowy, D.R., Schiller, J.T., 2003. Papillomaviruses infect cells via a clathrin-dependent pathway. Virology 307, 1–11.
Day, P.M., Baker, C.C., Lowy, D.R., Schiller, J.T., 2004. Establishment of papillomavirus infection is enhanced by promyelocytic leukemia protein (PML) expression. Proc. Natl. Acad. Sci. U.S.A. 101, 14252–14257.
Day, P.M., Gambhira, R., Roden, R.B., Lowy, D.R., Schiller, J.T., 2008. Mechanisms of human papillomavirus type 16 neutralization by L2 cross-neutralizing and L1 type-specific antibodies. J. Virol. 82, 4638–4646.
Finnen, R.L., Erickson, K.D., Chen, X.S., Garcea, R.L., 2003. Interactions between papillomavirus L1 and L2 capsid proteins. J. Virol. 77, 4818–4826.
Giroglou, T., Florin, L., Schäfer, F., Streeck, R.E., Sapp, M., 2001. Human papillomavirus infection requires cell surface heparan sulfate. J. Virol. 75, 1565–1570.
Hindmarsh, P.L., Laimins, L.A., 2007. Mechanisms regulating expression of the HPV 31 L1 and L2 capsid proteins and pseudovirion entry. Virol. J. 4, e19.
Howley, P.M., Lowy, D.R., 2001. Papillomaviruses and their replication, In: Lnipe, D.M., Howley, P.M. (Eds.), 4th ed. Fields Virology, Vol 2. Lippincott, Williams&Wilkins, Philadelphia, pp. 2197–2229.
Ishii, Y., Tanaka, K., Kanda, T., 2003. Mutational analysis of human papillomavirus type 16 major capsid protein L1: the cysteines affecting the intermolecular bonding and structure of L1-capsids. Virology 308, 128–136.
Ishii, Y., Kondo, K., Matsumoto, T., Tanaka, K., Shinkai-Ouchi, F., Hagiwara, K., Kanda, T., 2007. Thiol-reactive reagents inhibits intracellular trafficking of human papillomavirus type 16 pseudovirions by binding to cysteine residues of major capsid protein L1. Virol. J. 4, 110.
Kämper, N., Day, P.M., Nowak, T., Selinka, H.C., Florin, L., Bolscher, J., Hilbig, L., Schiller, J. T., Sapp, M., 2006. A membrane-destabilizing peptide in capsid protein L2 is required for egress of papillomavirus genomes from endosomes. J. Virol. 80, 759–768.
Kondo, K., Ishii, Y., Ochi, H., Matsumoto, T., Yoshikawa, H., Kanda, T., 2007. Neutralization of HPV16, 18, 31, and 58 pseudovirions with antisera induced by immunizing rabbits with synthetic peptides representing segments of the HPV16 minor capsid protein L2 surface region. Viroloy 358, 266–272.

Okun, M.M., Day, P.M., Greenstone, H.L., Booy, F.P., Lowy, D.R., Schiller, J.T., Roden, R.B., 2001. L1 interaction domains of papillomavirus L2 necessary for viral genome encapsidation. J. Virol. 75, 4332–4342.

Pastrana, D.V., Gambhira, R., Buck, C.B., Pang, Y.Y., Thompson, C.D., Culp, T.D., Christensen, N.D., Lowy, D.R., Schiller, J.T., Roden, R.B., 2005. Cross-neutralization of cutaneous and mucosal Papillomavirus types with anti-sera to the amino terminus of L2. Virology 337, 365–372.

Pyeon, D., Pearce, S.M., Lank, S.M., Ahlquist, P., Lambert, P.F., 2009. Establishment of human papillomavirus infection requires cell cycle progression. PLoS Pathog. 5, e1000318.

Richards, R.M., Lowy, D.R., Schiller, J.T., Day, P.M., 2006. Cleavage of the papillomavirus minor capsid protein, L2, at a furin consensus site is necessary for infection. Proc. Natl. Acad. Sci. U.S.A. 103, 1522–1527.

Schmitz, G., Müller, G., 1991. Structure and function of lamellar bodies, lipid–protein complexes involved in storage and secretion of cellular lipids. J. Lipid Res. 32, 1539–1570.

Smith, J.L., Campos, S.K., Wandinger-Ness, A., Ozbun, M.A., 2008. Caveolin-1-dependent infectious entry of human papillomavirus type 31 in human keratinocytes proceeds to the endosomal pathway for pH-dependent uncoating. J. Virol. 82, 9505–9512.

Spoden, G., Freitag, K., Husmann, M., Boller, K., Sapp, M., Lambert, C., Florin, L., 2008. Clathrin- and caveolin-independent entry of human papillomavirus type 16-involvement of tetraspanin-enriched microdomains (TEMs). PLoS ONE 3, e3313.

Yang, R., Yutzy 4th, W.H., Viscidi, R.P., Roden, R.B., 2003. Interaction of L2 with beta-actin directs intracellular transport of papillomavirus and infection. J. Biol. Chem. 278, 12546–12553.

Zhou, J., Gissmann, L., Zentgraf, H., Müller, H., Picken, M., Müller, M., 1995. Early phase in the infection of cultured cells with papillomavirus virions. Virology 214, 167–176.

zur Hausen, H., 2002. Papillomaviruses and cancer: from basic studies to clinical application. Nat. Rev. Cancer 2, 342–350.

Biased amplification of human papillomavirus DNA in specimens containing multiple human papillomavirus types by PCR with consensus primers

Seiichiro Mori,[1,4,5] Sari Nakao,[1,5] Iwao Kukimoto,[1] Rika Kusumoto-Matsuo,[1] Kazunari Kondo[2] and Tadahito Kanda[1,3]

[1]Pathogen Genomics Center, National Institute of Infectious Diseases, Shinjuku-ku, Tokyo; [2]NTT Medical Center Tokyo, Shinagawa-ku, Tokyo; [3]Center of Research Network for Infectious Diseases, Riken, Chiyoda-ku, Tokyo, Japan

(Received January 18, 2011/Revised March 2, 2011/Accepted March 2, 2011/Accepted manuscript online March 9, 2011)

Genotyping human papillomavirus (HPV) in clinical specimens is important because each HPV type has different oncogenic potential. Amplification of HPV DNA by PCR with the consensus primers that are derived from the consensus sequences of the *L1* gene has been used widely for the genotyping. As recent studies have shown that the cervical specimens often contain HPV of multiple types, it is necessary to confirm whether the PCR with the consensus primers amplifies multiple types of HPV DNA without bias. We amplified HPV DNA in the test samples by PCR with three commonly used consensus primer pairs (L1C1/L1C2+C2M, MY09/11, and GP5+/6+), and the resultant amplicons were identified by hybridization with type-specific probes on a nylon membrane. L1C1/L1C2+C2M showed a higher sensitivity than the other primers, as defined by the ability to detect HPV DNA, on test samples containing serially diluted one of HPV16, 18, 51, 52, and 58 plasmids. L1C1/L1C2+C2M failed to amplify HPV16 in the mixed test samples containing HPV16, and either 18 or 51. The three consensus primers frequently caused incorrect genotyping in the selected clinical specimens containing HPV16 and one or two of HPV18, 31, 51, 52, and 58. The data indicate that PCR with consensus primers is not suitable for genotyping HPV in specimens containing multiple HPV types, and suggest that the genotyping data obtained by such a method should be carefully interpreted. (*Cancer Sci*, doi: 10.1111/j.1349-7006.2011.01922.x, 2011)

Human papillomavirus (HPV), composed of an icosahedral capsid and a circular double-stranded DNA genome, is classified into more than 100 genotypes based on the nucleotide sequence homology of the *L1* gene encoding the major capsid protein.[1] The HPV types found in lesions of the skin and genital mucosa are grouped as cutaneous and genital HPVs, respectively. Of genital HPVs, 15 types (HPV16, 18, 31, 33, 35, 39, 45, 51, 52, 56, 58, 59, 66, 68, and 73) that have been found in cervical cancer are called high-risk HPVs[2] and the types, such as HPV6 and HPV11, that have been found in benign genital warts are called low-risk HPVs.[3]

For detection and genotyping of HPV DNA in the clinical specimens, such as cervical swabs and Pap smears, a part of the *L1* gene is amplified by PCR then grouped based on the susceptibility to various restriction enzymes, the binding capacity to type-specific probes, or the nucleotide sequences of the amplicons.[4] Several consensus primer pairs have been developed and used as standard primers for PCR-based genotyping of HPV in the clinical specimens. L1C1/L1C2+C2M was developed in 1991,[5] and has been used in more than 10 articles describing HPV prevalence in the Japanese population.[5–16] MY09/11[17] and GP5+/6+[18] were developed in 1989 and 1995, respectively, and have been used in numerous studies worldwide.[19] These primers are derived from the consensus sequences of the *L1* gene and the amplicons contain type-specific sequences. Recently new primers, PGMY09/11[20] and modified GP5+/6+ (MGP),[21] which are composed of several type-specific primers, were developed to improve the accuracy of HPV genotyping. The World Health Organization HPV Laboratory Network, which was founded to improve the quality of laboratory services for effective surveillance and monitoring of HPV vaccination impact, recommends PCR with PGMY09/11 followed by reverse blotting hybridization with type-specific probes, as a standard procedure for HPV genotyping.[22]

Recent studies showed that many HPV-positive women are infected with multiple genotypes.[23,24] Therefore, the methods capable of detecting and genotyping HPV DNA of multiple types in a single clinical specimen are necessary to know the precise prevalence of HPV types and the impact of HPV vaccines. As PCR does not always amplify different DNA fragments with equal efficiency, we examined whether PCR with consensus primers can amplify HPV DNA of multiple genotypes in a single sample without bias. We found that PCR with consensus primers sometimes results in mistyping.

Materials and Methods

Plasmids. The pUC plasmid containing the complete genome of HPV16, 18, 31, 51, or 52, or the *L1* gene of HPV58 was used. Purified plasmids were quantified with the NanoDrop ND-1000 (Thermo Fisher Scientific, Waltham, MA, USA). The copy numbers of HPV genomes were calculated from the concentration of plasmid expressed as molarities and Avogadro's number.

Clinical specimens. Cervical exfoliated cells were collected from outpatients who visited the NTT Medical Center Tokyo, with their informed consent. The study design and sample collection were approved by the institutional review board. One case of normal cytology, two cases of cervical intraepithelial neoplasia (CIN) grade 1, two cases of CIN2, two cases of CIN3, and one case of unknown cytology were selected for this study. DNA was purified using the QIAamp DNA blood kit (Qiagen, Hilden, Germany).

Polymerase chain reaction. Table 1 shows the sequences of primers used in this study: three consensus primer pairs, L1C1/L1C2+C2M,[5] MY09/11,[17] and GP5+/6+;[18] and two mixtures of type-specific primers, PGMY09/11[20] and modified GP5+/6+ (MGP).[21] Polymerase chain reaction amplification was done in a 50 μL reaction mixture containing 1× PCR buffer II (Life Technologies, Carlsbad, CA, USA), 1.25 units AmpliTaq Gold DNA polymerase (Life Technologies), and 50 ng cellular DNA extracted from human HaCaT cells. The 5′-end of either the forward or reverse primer was biotinylated. The concentrations of MgCl2, dNTPs, and primers, and the reaction temperature were adjusted to those used in the original article

[4]To whom correspondence should be addressed. E-mail: moris@nih.go.jp
[5]These authors contributed equally to this work.

doi: 10.1111/j.1349-7006.2011.01922.x
© 2011 Japanese Cancer Association

Table 1. Nucleotide sequences of primers used in this study

	Primer set	Forward (5′–3′)	Reverse (5′–3′)
Consensus primers	L1C1/L1C2+C2M	CGTAAACGTTTTCCCTATTTTTTT	TACCCTAAATACTCTGTATTG
			TACCCTAAATACCCTATATTG
	MY09/11	GCMCAGGGWCATAAYAATGG	CGTCCMARRGGAWACTGATC
	GP5+/6+	TTTGTTACTGTGGTAGATACTAC	GAAAAATAAACTGTAAATCATATTC
Multiple primers	PGMY09/11	GCACAGGGACATAACAATGG	CGTCCCAAAGGAAACTGATC
		GCGCAGGGCCACAATAATGG	CGACCTAAAGGAAACTGATC
		GCACAGGGACATAATAATGG	CGTCCAAAAGGAAACTGATC
		GCCCAGGGCCACAACAATGG	GCCAAGGGGAAACTGATC
		GCTCAGGGTTTAAACAATGG	CGTCCCAAAGGATACTGATC
			CGTCCAAGGGGATACTGATC
			CGACCTAAAGGGAATTGATC
			CGACCTAGTGGAAATTGATC
			CGACCAAGGGGATATTGATC
			GCCCAACGGAAACTGATC
			CGACCCAAGGGAAACTGGTC
			CGTCCTAAAGGAAACTGGTC
			GCGACCCAATGCAAATTGGT
	MGP	ACGTTGGATGTTTGTTACTGTGGTGGATACTAC	ACGTTGGATGGAAAAATAAACTGTAAATCATATTCCT
		ACGTTGGATGTTTGTTACCGTTGTTGATACTAC	ACGTTGGATGGAAAAATAAATTGTAAATCATACTC
		ACGTTGGATGTTTGTTACTAAGGTAGATACCACTC	ACGTTGGATGGAAATATAAATTGTAAATCAAATTC
		ACGTTGGATGTTTGTTACTGTTGTGGATACAAC	ACGTTGGATGGAAAAATAAACTGTAAATCATATTC
		ACGTTGGATGTTTGTTACTATGGTAGATACCACAC	ACGTTGGATGGAAAAATAAACTGCAAATCATATTC

MGP, modified GP5+/6+.

Fig. 1. Amplicons produced from the human papillomavirus (HPV)16*L1* gene by PCR with primers tested in this study. Both ends of amplicons are indicated by the nucleotide (nt) numbers of the HPV16*L1* gene. MGP, modified GP5+/6+.

describing the method.[5,17,18,20,21] Figure 1 shows the location of primers on the HPV16L1 ORF and the size of amplicons.

Reverse blotting hybridization. Reverse blotting hybridization was done as described previously.[22] Briefly, 15 μL denatured amplicons, of which the 5′-ends were labeled with biotin, were allowed to hybridize with the type-specific probes immobilized on a nylon membrane using the Miniblotter MN45 (Immunetics, Cambridge, MA, USA). The hybridized amplicon was detected using streptavidin–HRP (GE Healthcare Bio-Sciences, Piscataway, NJ, USA) and ECL detection reagents (GE Healthcare Bio-Sciences). The chemiluminescence was detected with the Light-Capture AE-6972 (ATTO, Tokyo, Japan). The intensities of dots were quantified by ImageJ software (National Institutes of Health, Bethesda, MD, USA). The specific density was calculated by the subtraction of the background from the integrated density. Samples showing the specific densities of more than 1000 intensity units were defined as positives.

The nucleotide sequences of type-specific probes for MY09/11, GP5+/6+, PGMY09/11, and MGP primers were described previously.[25,26] Type-specific probes for L1C1/L1C2+C2M primers were newly designed in this study. The nucleotide sequences were as follows: HPV16, 5′-GTTATTGTTAGGTTTTTTAA; HPV18, 5′-CCACCACCTGCAGGAACCCT; HPV31, 5′-AGGATTGTCAGATTTAGGTA; HPV51, 5′-TAGCAGCACGCGTTGAGGTT; HPV52, 5′-ACCATTACCACTACTGGTGT; and HPV58, 5′-TATTGTTATTGGGACTTTTG.

Real-time PCR. Copy numbers of HPV DNA in a clinical sample were determined by real-time PCR using type-specific primers and SYBR-green dye. A reaction mixture (20 μL) containing 2 μL sample, 10 μL Thunderbird SYBR qPCR Mix (Toyobo, Osaka, Japan), 0.4 μL ROX reference dye, and 0.9 μM each primer was subjected to PCR with the Applied Biosystems 7900HT (Life Technologies). The reaction was done in triplicate. The copy number was calculated with the standard curve obtained by using serially diluted HPV plasmids. The nucleotide sequences of type-specific primers are as follows: HPV16 forward, 5′-CAGAACCATATGGCGACAGC and reverse, 5′-GTACATTTTCACCAACAGCA; HPV18 forward, 5′-GATTATTTACAAATGTCTGCA and reverse, 5′-GCACAGTGTCACCCATAGTA; HPV31 forward, 5′-GATTATCTTAAAATGGTTGCT and reverse, 5′-GGACCGATTCACCAACCGTG; HPV51 forward, 5′-AGCTATGGATTTCGCTGCCC and reverse, 5′-AGCAAAGATTTGCTCCCTGC; HPV52 forward, 5′-GATTATTTGCAAATGGCTAGC and reverse, 5′-GGCACAGGGTCACCTAAGGTA; HPV58 forward, 5′-AGTGAACCTTATGGGGATAG and reverse, 5′-AAAGGTCATCCGGGA-

doi: 10.1111/j.1349-7006.2011.01922.x
© 2011 Japanese Cancer Association

CAGCC. Polymerase chain reaction with these primer sets amplified target HPV DNA without non-specific reaction. For example, PCR with the primers for HPV16 and a test sample containing HPV16 produced a single DNA fragment that formed a single peak in the dissociation curve.

Results

Amplification of HPV DNA in a test sample containing a single HPV genotype. Figure 2 shows the results of reverse blotting hybridization of the amplicons obtained by PCR from test samples (50 μL) containing 6, 60, 600, or 6000 copies of the plasmid having genomic DNA of HPV16, 18, 51, 52, and 58, all prevalent types among Japanese women, and 50 ng sheared human DNA. Three consensus primer pairs (L1C1/L1C2+C2M, MY09/11, and GP5+/6+) and two sets of mixed multiple primers (PGMY09/11 and MGP) were used for PCR. The biotinylated amplicons were allowed to hybridize with the type-specific probes immobilized on a nylon membrane and the biotin on the membrane was detected by streptavidin labeled with peroxidase.

Polymerase chain reaction with L1C1/L1C2+C2M produced detectable amplicons of HPV16, 18, 51, 52, and 58 from the samples containing 60, 6, 6, 60, and 60 copies of HPV DNA, respectively. Polymerase chain reaction with MY09/11 produced detectable amplicons of HPV16, 18, and 58 from the samples containing 600 copies of HPV DNA but did not produce detectable amplicons from the samples containing 6000 copies of HPV51 and 52. Polymerase chain reaction with GP5+/6+ produced detectable amplicons of HPV16, 18, 52, and 58 from the samples containing 60, 60, 6000, and 6000 copies, respectively, but failed to produce detectable amplicons from the sample containing 6000 copies of HPV51. Thus, PCR with L1C1/L1C2+C2M amplified HPV in the test samples more efficiently than the other PCR with the consensus primers.

Polymerase chain reaction with PGMY09/11 produced detectable amplicons of HPV16, 18, 51, 52, and 58 from the samples containing 6, 6, 60, 60, and 60 copies of HPV DNA, respectively. The PCR with MGP produced detectable amplicons of HPV16, 18, 51, 52, and 58 from samples containing 6, 60, 60, 6, and 600 copies of HPV DNA, respectively.

Amplification of HPV DNA in a mixed test sample containing HPV16, and either HPV18, 51, 52, or 58. Figure 3 shows the results of reverse blotting hybridization of the amplicons obtained by PCR from test samples containing 6000 copies of HPV16 and 6, 60, 600, and 6000 copies of either HPV18, 51, 52, or 58 and 50 ng sheared human DNA.

Polymerase chain reaction with L1C1/L1C2+C2M failed to amplify HPV16 DNA from the samples containing 6000 copies of HPV18 or 51 and the level of HPV16 amplicons was greatly reduced in the presence of 600 copies of HPV18 or 51. However, the amplification of HPV18 and 51 DNA was not influenced by the presence of 6000 copies of HPV16 DNA (Figs 2,3). The PCR with L1C1/L1C2+C2M amplified HPV16 DNA in the presence of HPV52 or 58 DNA. The data clearly indicate that amplification of HPV16 DNA by PCR with L1C1/L1C2+C2M was significantly interfered with by the presence of HPV18 or 51 DNA.

Polymerase chain reaction with MY09/11, GP5+/6+, PGMY09/11, or MGP amplified HPV16 DNA in the presence of HPV18, 51, 52, or 58 DNA but the level of HPV16 amplicons was reduced by co-existence of 6000 copies of HPV18 DNA. The PCR with GP5+/6+, PGMY09/11, or MGP produced reduced levels of HPV18, 52, or 58 amplicons in the co-existence of 6000 copies of HPV16 DNA (Figs 2,3).

Amplification of HPV DNA in clinical specimens containing two or three HPV genotypes. Table 2 shows the detection and genotyping of HPVs in clinical specimens using PCR with consensus primers. Eight clinical samples in which two or three HPV types had been detected by PCR with PGMY09/11 or MGP were selected, and the copy numbers of the detected HPV DNA in the samples were measured by real-time PCR using type-specific primers. Then the HPV in the samples was examined by PCR with L1C1/L1C2+C2M, MY09/11, or GP5+/6+. The HPV types detected with consensus primers are listed in decreasing order of amplicon levels.

In no. 165 containing HPV16 (16 000 copies), 18 (5200), and 31 (3100), HPV18 was detected by PCR with L1C1/L1C2+C2M but neither HPV16, which was three times more abundant than HPV18, nor 31 were detected. All three HPVs were detected by PCR with MY09/11. HPV16 and 18 were

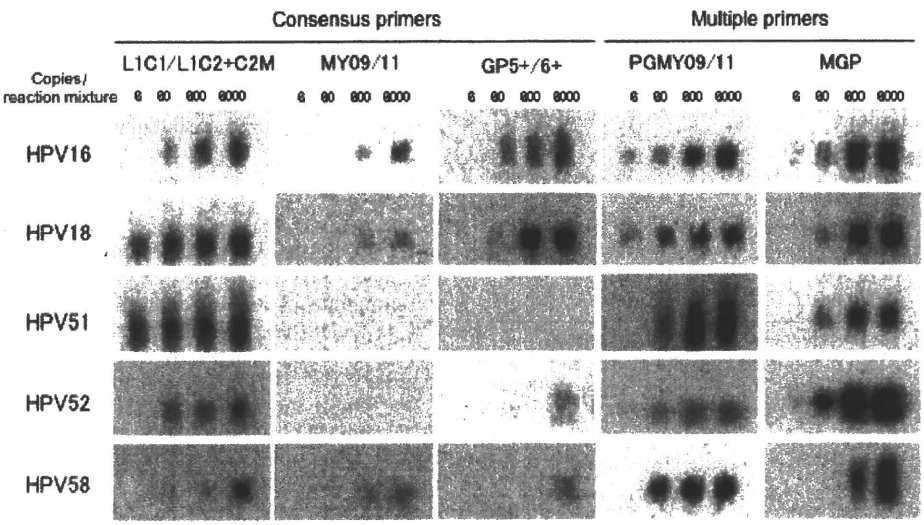

Fig. 2. Amplification of human papillomavirus (HPV) DNA in test samples containing HPV DNA of single genotype. The HPV DNA in the test sample was amplified by PCR with primers indicated. The test sample contained 6, 60, 600, or 6000 copies of plasmid DNA having HPV genomic DNA of the indicated type. The biotin-labeled amplified DNA fragments were hybridized with type-specific probes fixed on a membrane and reacted with streptavidin–HRP. MGP, modified GP5+/6+.

© 2011 Japanese Cancer Association

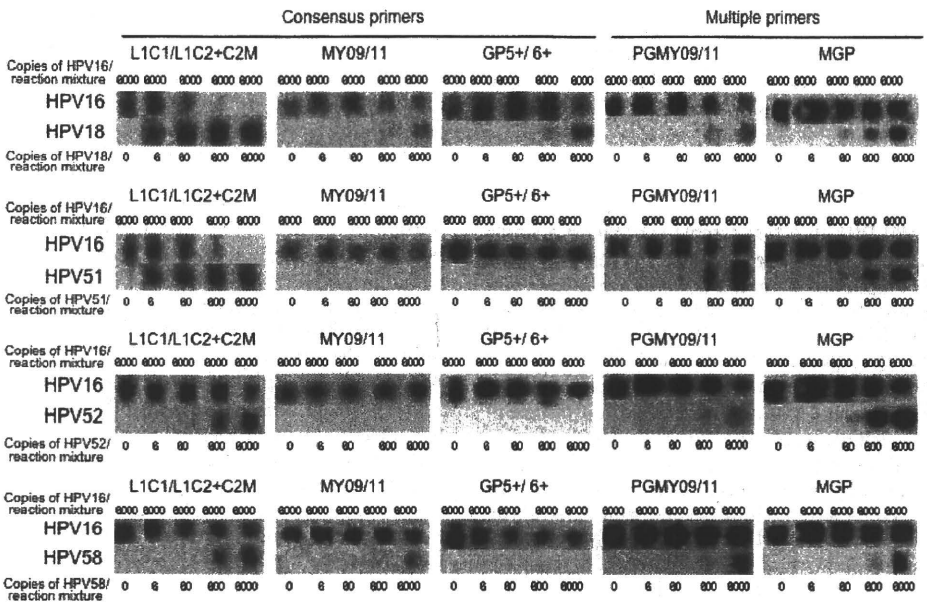

Fig. 3. Amplification of human papillomavirus (HPV) DNA in test samples containing HPV16 DNA and either HPV18, 51, 52, or 58 DNA. HPV DNA in the test sample was amplified by PCR with primers indicated. The test sample contained 6000 copies of HPV16 plasmid together with 6, 60, 600, or 6000 copies of HPV18, 51, 52, or 58 plasmid. The biotin-labeled amplified DNA fragments were hybridized with type-specific probes fixed on a membrane and reacted with streptavidin-horseradish peroxidase. MGP, modified GP5+/6+.

Table 2. Genotyping of clinical samples containing multiple types of human papillomavirus (HPV)

Sample no. (cytology)	Genotypes: copy numbers†	Consensus primers		
		L1C1/ L1C2+C2M	MY09/11	GP5+/6+
165 (CIN2)	16:16 000	18	18‡	16
	18:5200		16	18
	31:3100		31	
258 (CIN3)	52:1700	52	16	16
	16:1300	16	58	
	58:180	58		
352 (normal)	16:200		16	16
	52:25			
402 (CIN2)	52:7300	51	52	16
	51:120	52	16	
	16:110			
993 (CIN1)	16:5600	16	16	16
	52:3300	52		
996 (CIN1)	16:47 000	16	16	16
	52:25 000	52		
1061 (unknown)	18:4300	18	18	18
	16:290		16	16
1245 (CIN3)	16:78 000	58	58	16
	58:78 000	16	16	

†Genotypes detected using PGMY09/11 and modified GP5+/6+ primers. Copy numbers were determined by real-time PCR and expressed as copy numbers subjected to PCR for genotyping. ‡The HPV types detected with consensus primers are listed in decreasing order of amplicon levels.

detected by PCR with GP5+/6+ but HPV31, the least component, was not detected by PCR with GP5+/6+.

In no. 258 containing HPV52 (1700), 16 (1300), and 58 (180), all three HPVs were detected by PCR with L1C1/L1C2+C2M. HPV16 and 58 were detected by PCR with MY09/11 but HPV52, the most abundant type, was not detected. Only HPV16 was detected by PCR with GP5+/6+.

In no. 352 containing HPV16 (200) and 52 (25), neither HPVs were detected by PCR with L1C1/L1C2+C2M. Only HPV16 was detected by PCR with MY09/11 and PCR with GP5+/6+.

In no. 402 containing HPV52 (7300), 51 (120), and 16 (110), HPV16 was not detected by PCR with L1C1/L1C2+C2M. HPV16 and 52, but not HPV51, were detected by PCR with MY09/11. Only HPV16 was detected by PCR with GP5+/6+.

In no. 933 containing HPV16 (5600) and 52 (3300), and in no. 996 containing HPV16 (47 000) and 52 (25 000), HPV52 was not detected by PCR with MY09/11 and GP5+/6+.

In no. 1061 containing HPV18 (4300) and 16 (290), HPV16 was not detected by PCR with L1C1/L2C2+C2M.

In no. 1245 containing HPV16 (78 000) and 58 (78 000), HPV58 was not detected by PCR with GP5+/6+. Thus, amplification of HPV DNA in the clinical specimens containing multiple HPV genotypes by PCR with consensus primers was biased and sometimes caused misjudgment in typing.

Discussion

We evaluated HPV consensus primers for PCR amplification of HPV DNA in specimens containing multiple HPV types and concluded that PCR with consensus primers is not suitable for simultaneous amplification of multiple types of HPV DNA. The low sensitivity of HPV51 and 52 detection by PCR with MY09/11 and GP5+/6+ is consistent with previous reports.[20,21,27] Polymerase chain reaction with L1C1/L1C2+C2M, which amplified HPV DNA tested more efficiently than PCR with MY09/11 or GP5+/6+ (Fig. 2), failed to amplify HPV16 DNA when HPV18 or 51 DNA coexisted in the samples (Fig. 3, Table 2).

Polymerase chain reaction with L1C1/L1C2+C2M amplifies HPV18 and 51 DNA very efficiently, as shown in Figure 2. The resultant abundant HPV18 and 51 amplicons might inhibit reactions amplifying the other HPV types in the samples. Similarly, it is reported that interference in PCR was observed even

doi: 10.1111/j.1349-7006.2011.01922.x
© 2011 Japanese Cancer Association

between two closely related plant virus isolates that have identical binding sites for consensus primers, although the mechanism of the interference is not fully explained.[28]

As PCR with L1C1/L1C2+C2M has been used widely,[5–16] the biased amplification may have caused mistyping in the previous numerous studies of genotyping of clinical specimens. Previous studies using L1C1/L1C2+C2M showed that the rate of multiple infections among HPV-positive Japanese women was 10–20%.[15,16] In other countries, studies using PGMY09/11 showed that 30–45% of HPV-positive women were infected with multiple genotypes.[20,29–31] It is possible that reevaluation of HPV prevalence in Japanese women by using mixtures of type-specific primers, such as PGMY09/11 and MGP, increases the rate of multiple infections. The data of this study suggest that the genotyping data obtained by PCR with consensus primers should be carefully interpreted.

Acknowledgments

We acknowledge the World Health Organization's HPV Laboratory Network for technical transfer of reverse blotting hybridization into our laboratory. This work was supported by a grant-in-aid from the Ministry of Health, Labour and Welfare for the Third-Term Comprehensive 10-year Strategy for Cancer Control.

Disclosure Statement

The authors have no conflict of interest to declare.

References

1 Howley PM, Lowy DR. Papillomaviruses and their replication. In: Lnipe DM, Howley PM, eds. *Fields Virology*, Vol. 2, 4th edn. Philadelphia, PA: Lippincott, Williams and Wilkins, 2001; 2197–229.

2 Munoz N, Bosch FX, Castellsague X *et al.* Against which human papillomavirus types shall we vaccinate and screen? *Int J Cancer* 2004; **111**: 278–85.

3 Lacey CJ, Lowndes CM, Shah KV. Chapter 4: Burden and management of non-cancerous HPV-related conditions: HPV-6/11 disease. *Vaccine* 2006; **24**: S3/35–41.

4 Molijn A, Kleter B, Quint W, van Doorn LJ. Molecular diagnosis of human papillomavirus (HPV) infections. *J Clin Virol* 2005; **32**: S43–51.

5 Yoshikawa H, Kawana T, Kitagawa K, Mizuno M, Yoshikura H, Iwamoto A. Detection and typing of multiple genital human papillomaviruses by DNA amplification with consensus primers. *Jpn J Cancer Res* 1991; **82**: 524–31.

6 Iwasaka T, Matsuo N, Yokoyama M, Uchiyama K, Fukuda H, Sugimori H. Prospective follow-up of Japanese women with cervical intraepithelial neoplasia and various human papillomavirus types. *Int J Gynecol Obstet* 1998; **62**: 269–77.

7 Yoshikawa H, Nagata C, Noda K *et al.* Human papillomavirus infection and other risk factors for cervical intraepithelial neoplasia in Japan. *Br J Cancer* 1999; **80**: 621–4.

8 Maehama T, Asato T, Kanazawa K. Prevalence of HPV infection in cervical cytology-normal women in Okinawa, Japan, as determined by a polymerase chain reaction. *Int J Gynaecol Obstet* 2000; **69**: 175–6.

9 Maehama T, Asato T, Kanazawa K. Prevalence of human papillomavirus in cervical swabs in the Okinawa Islands, Japan. *Arch Gynecol Obstet* 2002; **267**: 64–6.

10 Masumoto N, Fujii T, Ishikawa M *et al.* Papanicolaou tests and molecular analyses using new fluid-based specimen collection technology in 3000 Japanese women. *Br J Cancer* 2003; **88**: 1883–8.

11 Asato T, Maehama T, Nagai Y, Kanazawa K, Uezato H, Kariya K. A large case-control study of cervical cancer risk associated with human papillomavirus infection in Japan, by nucleotide sequencing-based genotyping. *J Infect Dis* 2004; **189**: 1829–32.

12 Masumoto N, Fujii T, Ishikawa M *et al.* Dominant human papillomavirus 16 infection in cervical neoplasia in young Japanese women; study of 881 outpatients. *Gynecol Oncol* 2004; **94**: 509–14.

13 Maehama T. Epidemiological study in Okinawa, Japan, of human papillomavirus infection of the uterine cervix. *Infect Dis Obstet Gynecol* 2005; **13**: 77–80.

14 Takakuwa K, Mitsui T, Iwashita M *et al.* Studies on the prevalence of human papillomavirus in pregnant women in Japan. *J Perinat Med* 2006; **34**: 77–9.

15 Onuki M, Matsumoto K, Satoh T *et al.* Human papillomavirus infections among Japanese women: age-related prevalence and type-specific risk for cervical cancer. *Cancer Sci* 2009; **100**: 1312–6.

16 Matsumoto K, Oki A, Furuta R *et al.* Predicting the progression of cervical precursor lesions by human papillomavirus genotyping: a prospective cohort study. *Int J Cancer* 2010; doi: 10.1002/ijc.25630.

17 Manos MM, Ting Y, Wright DK, Lewis AJ, Broker TR, Wolinsky SM. The use of polymerase chain reaction amplification for the detection of genital human papillomaviruses. *Cancer Cell* 1989; **7**: 209–14.

18 de Roda Husman AM, Walboomers JM, van den Brule AJ, Meijer CJ, Snijders PJ. The use of general primers GP5 and GP6 elongated at their 3′ ends with adjacent highly conserved sequences improves human papillomavirus detection by PCR. *J Gen Virol* 1995; **76**: 1057–62.

19 Clifford GM, Smith JS, Plummer M, Muñoz N, Franceschi S. Human papillomavirus types in invasive cervical cancer worldwide: a meta-analysis. *Br J Cancer* 2003; **88**: 63–73.

20 Gravitt PE, Peyton CL, Alessi TQ *et al.* Improved amplification of genital human papillomaviruses. *J Clin Microbiol* 2000; **38**: 357–61.

21 Söderlund-Strand A, Carlson J, Dillner J. Modified general primer PCR system for sensitive detection of multiple types of oncogenic human papillomavirus. *J Clin Microbiol* 2009; **47**: 541–6.

22 World Health Organization, Department of Immunization, Vaccines and Biologicals. Human papillomavirus laboratory manual, 1st edn. 2009. Available from URL: http://www.who.int/biologicals/vaccines/hpv/en/index.html.

23 Mendez F, Munoz N, Posso H *et al.* Cervical coinfection with human papillomavirus (HPV) types and possible implications for the prevention of cervical cancer by HPV vaccines. *J Infect Dis* 2005; **192**: 1158–65.

24 Schmitt M, Dondog B, Waterboer T, Pawlita M, Tommasino M, Gheit T. Abundance of multiple high-risk human papillomavirus (HPV) infections found in cervical cells analyzed by use of an ultrasensitive HPV genotyping assay. *J Clin Microbiol* 2010; **48**: 143–9.

25 Gravitt PE, Peyton CL, Apple RJ, Wheeler CM. Genotyping of 27 human papillomavirus types by using L1 consensus PCR products by a single-hybridization, reverse line blot detection method. *J Clin Microbiol* 1998; **36**: 3020–7.

26 Schmitt M, Bravo IG, Snijders PJ, Gissmann L, Pawlita M, Waterboer T. Bead-based multiplex genotyping of human papillomaviruses. *J Clin Microbiol* 2006; **44**: 504–12.

27 Chan PK, Cheung TH, Tam AO *et al.* Biases in human papillomavirus genotype prevalence assessment associated with commonly used consensus primers. *Int J Cancer* 2006; **118**: 243–5.

28 Rosner A, Maslenin L. Interference in PCR: transcription amplifications of mixed PVY isolates. *Plant Prot Sci* 2005; **41**: 125–31.

29 Coutlée F, Gravitt P, Kornegay J *et al.* Use of PGMY primers in L1 consensus PCR improves detection of human papillomavirus DNA in genital samples. *J Clin Microbiol* 2002; **40**: 902–7.

30 Klug SJ, Hukelmann M, Hollwitz B *et al.* Prevalence of human papillomavirus types in women screened by cytology in Germany. *J Med Virol* 2007; **79**: 616–25.

31 van Doorn LJ, Quint W, Kleter B *et al.* Genotyping of human papillomavirus in liquid cytology cervical specimens by the PGMY line blot assay and the SPF(10) line probe assay. *J Clin Microbiol* 2002; **40**: 979–83.

© 2011 Japanese Cancer Association

International Journal of Gynecological Pathology
30:30–35. Lippincott Williams & Wilkins. Baltimore
© 2010 International Society of Gynecological Pathologists

Original Article

Rsf-1 (HBXAP) Expression is Associated With Advanced Stage and Lymph Node Metastasis in Ovarian Clear Cell Carcinoma

Daichi Maeda, M.D., Xu Chen, M.D., Bin Guan, Ph.D., Shunsuke Nakagawa, M.D., Ph.D., Tetsu Yano, M.D., Ph.D., Yuji Taketani, M.D., Ph.D., Masashi Fukayama, M.D., Ph.D., Tian-Li Wang, Ph.D., and Ie-Ming Shih, M.D., Ph.D.

Summary: Ovarian clear cell carcinoma (CCC) is a unique type of ovarian cancer characterized by distinct clinicopathological and molecular features. CCC is considered to be a highly malignant disease because it is resistant to conventional chemotherapy, and when presented at advanced stages, it has a dismal overall survival. Identifying and characterizing biomarkers associated with its malignant behavior is fundamental toward elucidating the mechanisms underlying its aggressive phenotype. In this study, we performed immunohistochemical analysis on 89 CCCs to assess their expression of Rsf-1 (HBXAP), a chromatin-remodeling gene frequently amplified and overexpressed in several types of human cancer. We found that 73 (82%) of the 89 CCCs expressed Rsf-1 and most importantly, there was a statistically significant correlation between Rsf-1 immunostaining intensity and the 2 disease parameters: advanced stage ($P=0.008$) and status of retroperitoneal lymph node metastasis ($P=0.023$). However, there was no correlation between Rsf-1 expression and patient age, peritoneal tumor dissemination, or overall survival. In conclusion, a higher expression level of Rsf-1 is associated with advanced clinical stage and lymph node metastasis in CCC. Our data suggest that Rsf-1 participates in tumor progression in CCC, and indicates that the contribution of Rsf-1 to disease aggressiveness deserves further study. **Key Words:** Rsf-1–HBXAP–Ovarian cancer—Clear cell carcinoma.

Ovarian clear cell carcinoma (CCC) represents less than 10% of ovarian cancers in the United States, but occurs more frequently in Asian women (1,2). Multivariate analysis on a large series of CCC shows that women with CCC present at a younger age and at earlier clinical stages as compared with high-grade (conventional) serous carcinoma, the most common and lethal type of ovarian cancer (1). Approximately 50% of CCCs present as stage I diseases (3,4), and despite being diagnosed at an early stage, are generally considered to be highly malignant (5). Morphologic and molecular studies have shown that many CCCs develop in a stepwise manner from endometriosis through atypical endometriosis to overt CCC (6–10). In fact, CCC is the most common ovarian carcinoma associated with endometriosis. There has been increased enthusiasm for identifying markers that are predictive of the clinical outcome in CCC patients. This is because CCC typically presents with stage I or II disease, and prognostic markers could have an impact on clinical decision making in the management of CCC patients, such as administration of adjuvant

From the Department of Pathology (D.M., X.C., B.G., I-M.S.); Departments of Gynecology and Obstetrics and Oncology (D.M., T-L.W., I-M.S.), Johns Hopkins Medical Institutions, Baltimore, Maryland; Department of Pathology (D.M., M.F.); and Department of Obstetrics and Gynecology (S.N., T.Y., Y.T.), Graduate School of Medicine, the University of Tokyo, Tokyo, Japan.

This study was supported by NIH/NCI Grant CA129080 and the International Training Program from the Japan Society for the Promotion of Science.

Address correspondence and reprint requests to Ie-Ming Shih, MD, PhD, Johns Hopkins Medical Institutions, 1550 Orleans street, CRB-2, room: 305, Baltimore, Maryland 21231. E-mail: ishih@jhmi.edu.

DOI: 10.1097/PGP.0b013e3181e9a319

chemotherapy. For example, IGF2BP3 (IMP3) expression has been reported to be an independent marker of reduced disease-specific survival in CCC, but not in high-grade serous or endometrioid carcinomas of the ovary (11). Similarly, enhanced expression of annexin A4 in CCC and its association with chemoresistance to carboplatin have been recently reported (12).

To further identify markers that are associated with poor prognosis in CCC and to explore the molecular mechanisms that account for the aggressive behavior of CCC, we determined the correlation between immunoreactivity of Rsf-1, also known as HBXAP, and clinical outcome in primary CCCs. We focused on Rsf-1 (HBXAP) because the encoded protein participates in chromatin remodeling, and this gene has been identified as an amplified gene with a tumor-promoting potential in several types of neoplastic diseases including ovarian high-grade serous carcinoma (13–15). Our analysis showed that the higher expression levels of Rsf-1 (HBXAP) were associated advanced stage disease and retroperitoneal lymph node metastasis. This study provides new evidence of the biological significance of Rsf-1 expression in CCC.

MATERIALS AND METHODS

Tissue Samples

Formalin-fixed and paraffin-embedded CCC tissues were obtained from the Department of Pathology at the University of Tokyo Hospital. A total of 89 cases of primary CCCs were retrieved from the archives, and hematoxylin and eosin-stained slides were reviewed to confirm the diagnosis based on the most recent criteria of the World Health Organization. The CCC tissues were arranged in tissue microarrays (Beecher Instruments, Silver Spring, MD) with duplicate 2 mm tissue cores obtained from the tumor area in each CCC. The collection of clinical specimens was in compliance with the guidelines of tissue procurement at the University of Tokyo Hospital.

Clinical Information of Patients With Ovarian CCC

We reviewed the medical records of all the 89 CCC patients; data obtained included demographics, age at the time of diagnosis, preoperative diagnosis, clinical stage, and survival time after treatment. None of the patients underwent preoperative chemotherapy or radiotherapy. The correlations of Rsf-1 expression with the following clinical variables were evaluated: age, stage of carcinoma (stage I/II vs. stage III/IV), peritoneal dissemination, retroperitoneal lymph node metastasis, and death rate. The stage of carcinoma was assessable in 67 cases in which the appropriate staging procedures were performed; the remaining 22 cases were not included in the staging analysis because of either incomplete surgical procedures or missing data. Staging was in accordance with the standards of the International Federation of Gynecology and Obstetrics. Comprehensive evaluation of peritoneal dissemination that included microscopic examination of the omentum, peritoneal wall and mesentery soft tissues was performed in 79 cases. Retroperitoneal lymph node dissection was performed in 70 cases. Follow-up information included overall survival and cancer-related death. The follow-up interval was calculated from the date of surgery to the date of death or last clinical evaluation. The mean follow-up interval was 50 months (range, 1–196 mo).

Immunohistochemistry

The method of immunohistochemistry and scoring of immunoreactivity for Rsf-1 expression were described earlier (13,14). In brief, 4 μm sections were cut from the tissue microarray blocks. Antigen retrieval was performed on the deparaffinized sections by steaming them in citrate buffer (pH 6.0). A monoclonal anti-Rsf-1 antibody, clone 5H2/E4 (Upstate, Lake Placid, NY) was used at an optimal dilution of 1:2000 as determined earlier (13,14) and a monoclonal anti-NAC1 antibody was used at a dilution of 1:250 (16). The sections were incubated with the antibodies for 2 hours at room temperature, followed by the EnVision+ System (Dako, Carpinteria, CA) using the peroxidase method. An isotype-matched control antibody (MN-4) was used in parallel (17). Our earlier studies had shown that the distribution of Rsf-1 immunoreactivity was always homogeneous within a tumor; therefore, we used an intensity score ranging from 0 to 4+ to evaluate Rsf-1 immunoreactivity in tumors as described earlier (14). A positive reaction for both Rsf-1 and NAC1 was defined as discrete localization of the chromogen in the nuclei. The tissues were scored in a blinded manner without the knowledge of clinical information.

Rsf-1 Gene Knockdown Using Small Hairpin RNA

Ovarian clear cell adenocarcinoma cell lines, ES2 and JHOC5, were used in this study. ES2 was

obtained from the American Type Culture Collection (Rockville, MD); JHOC5 was a gift from Dr Kentaro Nakayama, Shimane University, Japan. Both the cell lines used in this study were cultured in RPMI 1640 containing 5% fetal bovine serum.

To confirm the specificity of the anti-Rsf-1 antibody used for immunohistochemistry, we performed Rsf-1 knockdown by transduction of 2 small hairpin RNAs (shRNA) and evaluated the knockdown efficiency by Western blot analysis. The antibody specificity was indicated by reduced protein expression corresponding to Rsf-1 after the gene knockdown based on the western blot analysis using the same anti-Rsf-1 antibody as used in immunohistochemistry. We used a lentivirus carrying the Rsf-1 shRNA sequence templates (CCGGCCAGTTCTGAACTTTGAAGATCTCGAGATCTTCAAAGTTCAGAACT) and (CCGGCTTCTGAGACAAAGGGTTCTACTCGAGTAGAACCCTTTGTCTCAGA), and a control shRNA sequence template, which were inserted into the lentiviral plasmid (pLKO.1-puro). The cells were washed and harvested 24 hours after transfection for protein and mRNA extraction.

For Western blot analysis, the protein lysates were separated by 4% to 20% Tris-glycine gel electrophoresis and transferred onto polyvinylidene difluoride membranes using a semidry apparatus (Bio-Rad). After blocking, the membranes were incubated with the anti-Rsf-1 (clone 5H2/E4) primary antibody at 4°C overnight followed by incubation with horseradish peroxidase-conjugated secondary antibody. Protein bands were detected with Amersham ECL Western blotting detection reagents (GE Healthcare). Antibody reacting to anti-glyceraldehyde-3-phosphate dehydrogenase was used to evaluate the amount of glyceraldehyde-3-phosphate dehydrogenase as a loading control. Western blot analysis showed a reduced protein band corresponding to Rsf-1 in the cells transfected with Rsf-1 shRNA as compared with the control shRNA-transfected cells, indicating the specificity of the anti-Rsf-1 antibody (Fig. 1).

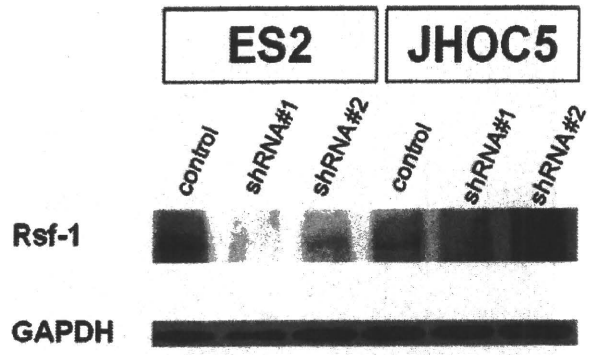

FIG. 1. Rsf-1 expression in ovarian clear cell carcinoma cell lines, ES2 and JHOC5. Western blot analysis showed a reduced protein band corresponding to Rsf-1 protein in the Rsf-1-specific shRNA-transfected cells as compared with the control shRNA-transfected cells, indicating the specificity of the anti-Rsf-1 antibody. GAPDH indicates glyceraldehyde-3-phosphate dehydrogenase.

Statistical Analysis

Statistical analysis was performed using the χ^2 test. Overall survival of the CCC cases was calculated using the Kaplan-Meier method, and statistical analyses were performed using the log-rank test. Statistical analyses were performed using the StatView 5.0 software (SAS Institute, Cary, NC) and a $P<0.05$ was considered statistically significant.

RESULTS

Expression of Rsf-1 in Ovarian CCCs

Results of Rsf-1 immunohistochemistry in CCCs are summarized in Table 1. Rsf-1 immunoreactivity was detected exclusively in the nuclei of almost all the tumor cells. Positive immunoreactivity of Rsf-1 was observed in 73 (82%) of the 89 cases. Specifically, 16 (18%), 53 (60%), and 19 (21%) of the 89 cases had a staining score of 0, 1+, and 2+, respectively. Only 1 case exhibited intense nuclear staining (3+). Histologic features in the representative cases with different Rsf-1 immunostaining intensities including 0, 1+, and 2+ are shown in Figure 2. There was no correlation between Rsf-1 expression and the histological pattern and nuclear atypia of the CCC cases.

Correlation of Rsf-1 Expression With Clinical Features

As Rsf-1 expression has been reported to play a tumor-promoting role in ovarian cancer, we analyzed the possible correlation of Rsf-1 expression with clinical characteristics in CCC (Table 2). Statistically significant correlations were observed between Rsf-1 immunostaining intensity (score > 1) and lymph

TABLE 1. *Rsf-1 expression in ovarian clear cell carcinoma*

Immunostaining intensity score	No. cases	%
0	16	18
1+	53	60
2+	19	21
3+	1	1
4+	0	0
Total	89	100

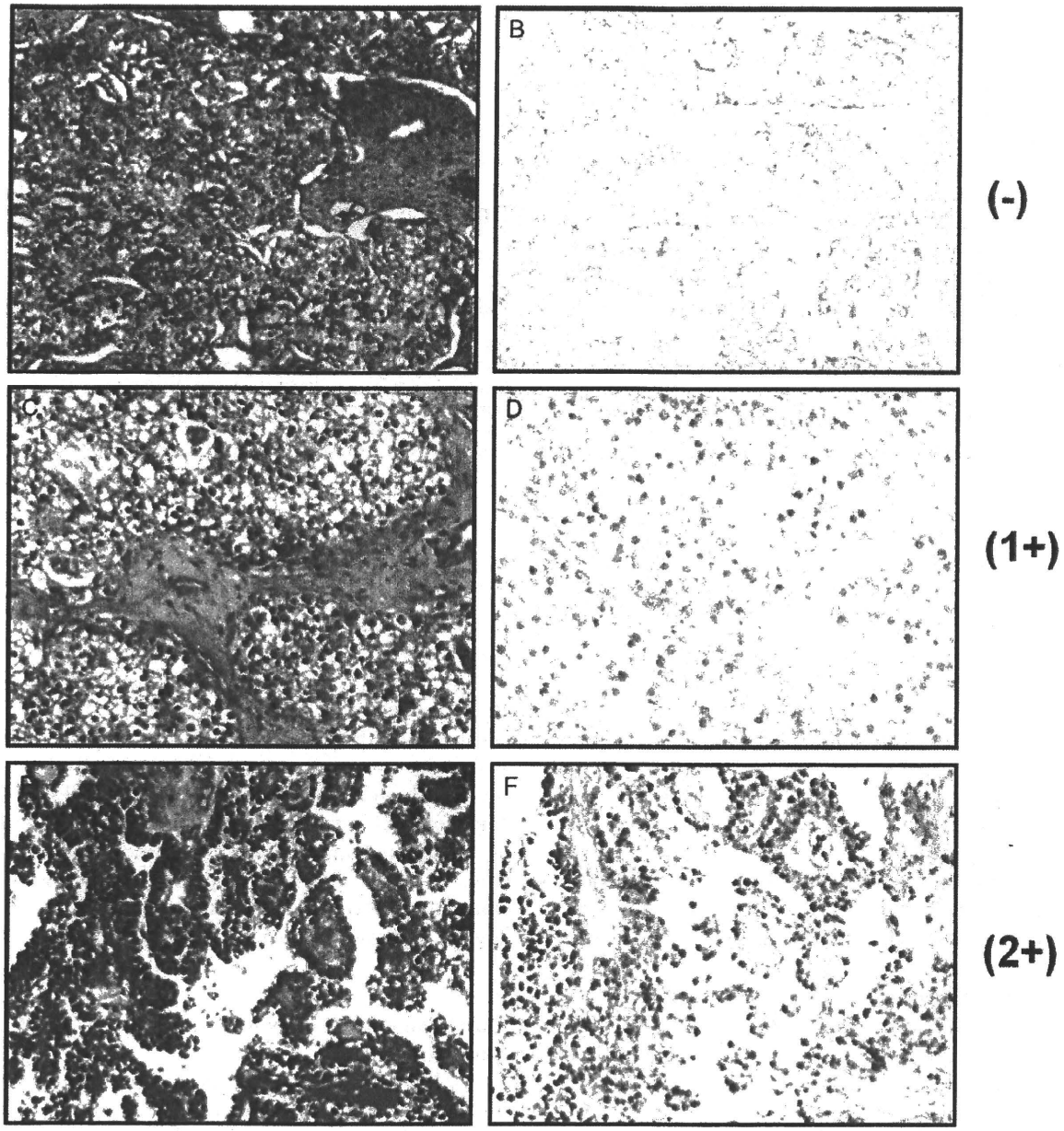

FIG. 2. Rsf-1 immunoreactivity in representative ovarian clear cell carcinomas. (A, B) Microscopic view of an ovarian clear cell carcinoma showing negative immunoreactivity for Rsf-1. (C, D) A case of ovarian clear cell carcinoma with 1+ immunostaining intensity for Rsf-1. (E, F) A clear cell carcinoma with 2+ immunoreactivity for Rsf-1. A, C, and E: hematoxylin and eosin-stained sections; B, D, and F: Rsf-1-stained sections.

node involvement ($P=0.023$). Furthermore, Rsf-1 immunostaining intensity (score >1) was associated with advanced stage disease (stage III/IV) ($P=0.0088$). In fact, none of the Rsf-1-negative cases presented at an advanced stage. The frequency of peritoneal dissemination was higher in the Rsf-1-positive cases (12 of 65) compared with the Rsf-1-negative cases (1 of 14), but the difference was not statistically significant ($P=0.3$). As a control we also assessed the expression of Nacl, a nuclear protein involved in transcription regulation, in the same set of CCCs. We found that there was no significant association between Nacl expression and any clinical feature including presentation stage or lymph node metastasis status ($P>0.1$) (data not shown). Kaplan-Meier analyses were performed to determine if there was a correlation between Rsf-1 expression and clinical outcome. We first assessed the association